ANALYSIS OF PROCESS PARAMETERS INVOLVED IN DRILLING OF CARBON FIBER REINFORCED EPOXY CLAY NANOCOMPOSITES

A

Thesis Report

submitted in partial fulfillment of the requirement for the award of the degree of

MASTER OF ENGINEERING
IN
CAD/CAM & ROBOTICS

Submitted By

GURTEJ SINGH

Roll No. 801181011

Under the Guidance of

Mr. BIKRAMJIT SHARMA
Assistant Professor
Thapar University, Patiala

Dr. VINOD KUMAR SINGLA
Associate Professor
Thapar University, patiala

MECHANICAL ENGINEERING DEPARTMENT

THAPAR UNIVERSITY, PATIALA-147004, INDIA

JULY, 2013

CERTIFICATE

This is to be certify that the thesis entitled **"ANALYSIS OF PROCESS PARAMETERS INVOLVED IN DRILLING OF CARBON FIBER REINFORCED EPOXY CLAY NANOCOMPOSITES"** is authentic record of my study carried out as requirement for the award of degree of **Master of Engineering** in **CAD/CAM & Robotics** at **Thapar University, Patiala** under the supervision of **Dr. Vinod Kumar Singla**, Associate Professor and **Mr. Bikramjit Sharma**, Assistant Professor, Department of Mechanical Engineering, Thapar University, Patiala during July 2011 to July 2013. The matter embodied in this report has not been submitted in part or full to any other university or institute for award of any degree.

Dated: 15/7/13

Gurtej Singh

Gurtej Singh

It is certified that the above statement made by the student is correct to best of my knowledge and belief.

Dr. VINOD KUMAR SINGLA
Associate Professor
Mechanical Engineering Department
Thapar University, Patiala-147004

MR. BIKRAMJIT SHARMA
Assistant Professor
Mechanical Engineering Department
Thapar University, Patiala-147004

Countersigned By

Dr. AJAY BATISH
Professor & Head
Mechanical Engineering Department
Thapar University, Patiala-147004

Dr. S. K. MOHAPATRA
Dean of Academic Affairs
Thapar University, Patiala-147004

ACKNOWLEDGEMENT

With deep sense of gratitude I express my sincere thanks to my guides, **Dr. Vinod Kumar Singla and Mr. Bikramjit sharma** for their valuable guidance, proper advice and constant encouragement during this report work. I found his guidance to be extremely valuable. I also feel very much obliged to **Dr. Ajay Batish,** Professor & Head, of Mechanical Engineering Department.

I would also like to thank all the members and employees of Mechanical Engineering Department, Thapar University, Patiala for their everlasting support.

I am also thankful to my friends for their cooperation. I would like to extend my gratitude to all those persons who directly or indirectly helped me in process and completion of this work.

GURTEJ SINGH

ABSTRACT

Carbon fiber reinforced epoxy composites find application in many fields due to their high specific strength, specific modulus and anticorrosion properties. In order to join different components by using fasteners, drilling operation is performed in composites. Drilling induces several imperfections in structures - Delamination, fiber pullout, matrix cracking, debonding etc. In the present work epoxy modified with Cloisite 30B® nanoclay (mixed in different concentrations 0.5wt%, 2wt%, 3wt% of resin) and unidirectional carbon fibers are used to manufacture laminates by hand layup method. Taguchi's design of experiment is used to analyze the degradation in properties considering different parameters involved in drilling. The input parameters considered are drill geometry: , feed:, speed: and nanoclay content. The response: Residual tensile strength, bearing strength and delamination are analysed using analysis of Variance (ANOVA) technique. The variation in nanoclay concentration and drill geometry have strongly affected the residual tensile strength and the bearing strength. The Delamination in composites has reduced with the use of twist drill.

TABLE OF CONTENTS

LIST OF FIGURES

LIST OF TABLES

ABBREVATIONS

CFRP	Carbon Fiber Reinforced Composites
OMMT	Montmorillonite Organoclay
SEM	Scanning Electron Microscope
ANOVA	Analysis Of Variance
DOE	Design Of Experiment
DOF	Degree Of Freedom
S/N	Signal to Noise Ratio
UTM	Universal Testing Machine

NOTATIONS

F_d	Delamination Factor
D_{max}	Maximum Delaminated Diameter
A	Feed
B	Speed
C	Nanoclay
D	Drill Geometry
C×D	Nanoclay × Drill Geometry
OA	Orthogonal Array
SS	Sum Of Squares
d	Diameter Of Hole
t	Thickness Of Specimen

CHAPTER 1 INTRODUCTION

1. Composites

A composite material is a macroscopic combination of two or more distinct materials, having a recognizable interface between them. Composites can be both natural and synthetic (or man-made). Synthetic or advanced composites are extensively used in industries, defence, aerospace, marine, civil structures etc. An advanced composite is made up of two constituents: matrix and reinforcement. The matrix material surrounds and supports the reinforcement materials by maintaining their relative positions. The reinforcements impart their special mechanical and physical properties to enhance the matrix properties.

Composites have wide range of applications. Composites are used in structural, electrical, thermal, building works, road transports, rail transports, marine transports, space transports and sports applications. Modern composite materials are usually optimized to achieve a particular balance of properties for a given range of applications.

1.1 Reinforcement

Reinforcement are used to provide the strength to composites and take most of the loading. Reinforcement materials are used in the form of continuous fibers, short fibers, particulate. Continuous fibers are materials that have one very long axis with a very high length to diameter/thickness ratio and are often circular or near circular in shape. Fibers have significantly higher strength and stiffness in the length direction than in the other directions. Thus fibers are most commonly used for the reinforcement of a softer matrix. The most commonly used composite fiber is discussed below.

1.1.1 Carbon Fiber

Carbon fiber, alternatively graphite fiber, carbon graphite is a material consisting of fibers about 5–10 μm in diameter and composed mostly of carbon atoms. The carbon atoms are bonded together in crystals that are more or less aligned parallel to the long axis of the fiber. The crystal alignment gives the fiber high strength-to-volume ratio

(makes it strong for its size). Several thousand carbon fibers are bundled together to form a tow, which may be used by itself or woven into a fabric.

The properties of carbon fibers, such as high stiffness, high tensile strength, low weight, high chemical resistance, high temperature tolerance and low thermal expansion, make them very popular in aerospace, civil engineering, military, and motor sports, along with other competition sports. However, they are relatively expensive when compared to similar fibers, such as glass fibers or plastic fibers.

Carbon fibers are usually combined with other materials to form a composite. In this case the composite consists of two parts; a matrix and a reinforcement. In CFRP the reinforcement is carbon fiber, which provides the strength. The matrix is usually a polymer resin, such as epoxy, to bind the reinforcements together. When combined with a plastic resin and wound or molded it forms carbon fiber reinforced plastic (often referred to as carbon fiber) which has a very high strength-to-weight ratio, and is extremely rigid although somewhat brittle.

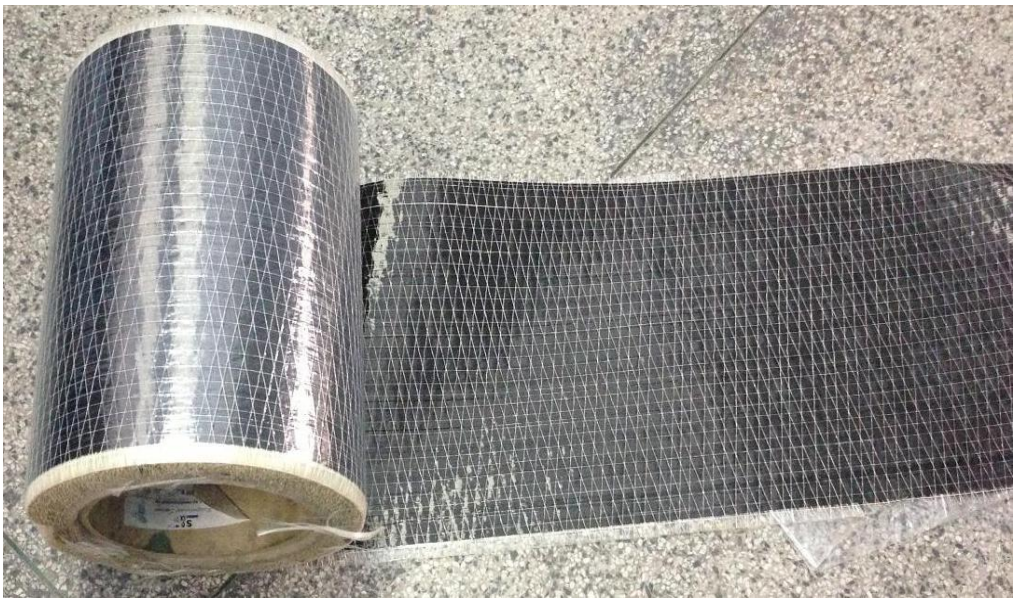

Fig: 1.1 Carbon Fiber

1.2 Matrix

The matrix material is used to bind the reinforcements so as to provide the shape to composites and transfer the loads to fiber strands protect them from abrasion and adverse environmental conditions. Matrix may be made from metals, ceramics or

polymers. It may be pure , or mixed with other materials (additives) to enhance its properties. The various functions of the matrix phase are given below:-

1. Matrix material holds the fibres together.
2. It protects the fibres from environment.
3. It distributes the loads evenly between the fibres so that all fibres are subjected to same amount of strain.
4. It enhances transverse properties of laminates.
5. It improves impact and fracture resistance of the component.

In 1946, the first industrially-produced epoxy resin was introduced to market. Since then, the use of thermosetting polymers has steadily increased. The wide range of epoxy resin applications includes: coating, electrical, automotive, marine, aerospace and civil infrastructure as well as tool fabrication and pipes and vessels in the chemical industry. Due to their low density of around 1.3 g/cm and good adhesive and mechanical properties, epoxy resin became a promising material for high performance applications in the transport industry, usually in the form of composite materials such as fiber composite or in honeycomb structures. In the aerospace industry, epoxy composites material can be found in various part of the body and structure of military and civil aircrafts, with the number of applications on the rise. A recent approach to improve and diversify polymer properties in the aerospace industries is through the dispersion of nanometer-scaled fillers in the polymer matrix.

1.3 Nanoclay

Clay as nanoparticles such as smectic clays (e.g. montmorillonite) are incorporated into polymers to form resulting polymer nanocomposite, which may possess unique electrical, mechanical and optical properties.

The presence of clay as filler strengthen the mechanical properties of Polymers even at low concentration of filler loading of filler. Partly because of their aspect ratios and high surface areas, the clay particles, if properly dispersed in the polymer matrix at a loading level of 1 to 5 wt. %, impart unique combinations of physical and chemical properties that make these nanocomposites attractive for making films and coatings for a variety of industrial applications. Relative to the unmodified polymer, the polymer/clay nanocomposites may exhibit improvemenjts in strength, modulus, and

toughness, tear, fire resistance, and lower thermal expansion and permeability to gases while retaining a high degree of optical transparency [www.techbriefs.com].

The most common type of nanoclay is montmorillonite (MMT), a layered alumino silicate in the smectite family of clay. Unlike clay minerals such as talc and mica that have been used as fillers for years, MMT can be delaminated and dispersed into an individual layers only one nanometer thick by about 70 nm to 150 nm across. Some of the commercially available organically modified montmorillonite nanoclay are cloisite 30B, cloisite 15A etc. Figure 1.2 shows structures of polymer-clay composites.

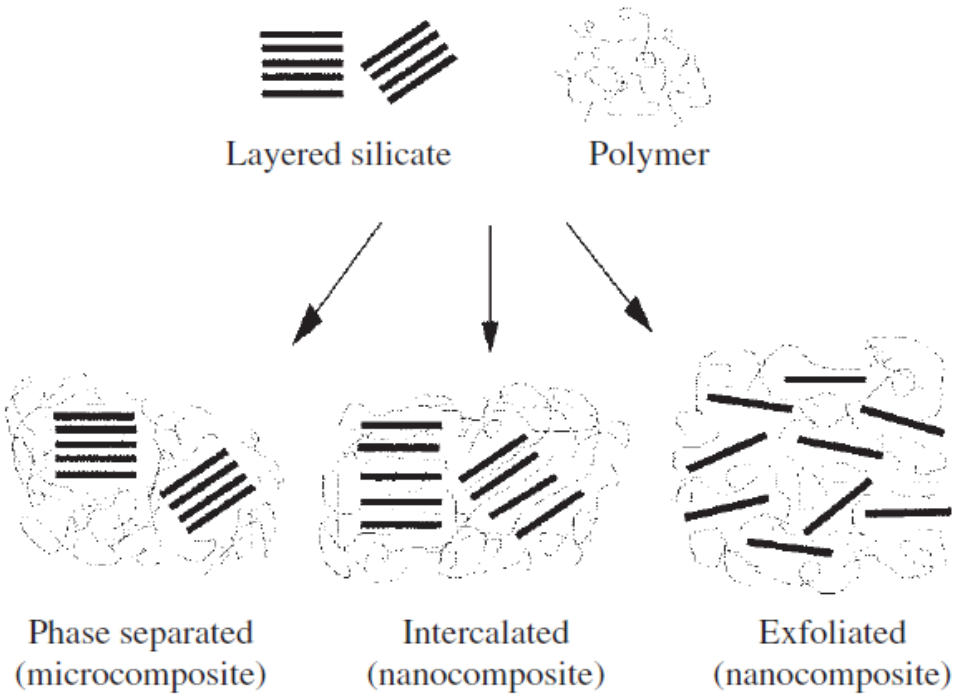

Fig: 1.2 Three structures of polymer-clay composites [23]

1. Phase separated dispersion, in which the polymer is unable to to penetrate between the layers of the silicate particles a conventional composite is formed.
2. Intercalated dispersion, in which one or more polymer molecules are intercalated between the silicate layers.
3. In exfoliated dispersion the silicate layers are completely delaminated and the silicate layers do not show any periodicity in their arrangement and uniformly dispersed in the polymer matrix.

2. Drilling in composites

2.1 Introduction

Drilling involves the removal of material from a work piece such that a hole is obtained. The holes created are used primarily for fastening components. Drilling is often used in the machining of composites, because of readily available machinery and it is simply more cost effective than the more advanced method like laser beam cutting. Drilling is performed to a large variety of materials in different industries, but had been mostly studied for metals cutting. Drilling performance depends on the materials involved, the drill geometry, the cutting parameters (spindle speed and the axial feed rate) and the process conditions (i.e. cooling, lubricant, fixturing etc.).

2.2 Damage in composites due to drilling

The failure modes of composites after drilling composite can be matrix cracking, fiber breakage, fiber pullout, delamination and debonding and the most critical delamination around the drill hole.

2.2.1 Delamination can be defined as the separation of the layers of material in a laminate. It can occur at any time in the life of a laminate for various reasons and has various effects. It can effect the tensile strength performance depending on the region of delamination or reduction in the durability of the composite material. Some of reasons for the occurrence of delamination are the high feed rate, rapid tool wear and power. Delamination is an internal defect and in most cases is not visible with the naked eye. Solutions like C-Scan, X-Ray computerized tomography, shadow laser based imaging technique, scanning technique are available for detecting delamination, but they are expensive and time consuming. There are two mechanism of delamination which occurs at both entry and exit point. At the point of entry, delamination is usually known as the peel up of the material. At the exit point, delamination occurs when the drill bit tries to push through the material.

Peel-up occurs as the drill enters the laminate and is shown in Fig. 2.1(a). After the cutting edge of the drill makes contact with the laminate, the cutting force acting in the peripheral direction is the driving force for delamination. It generates a peeling force in the axial direction through the slope of the drill flute results in separating the laminas from each other forming a delamination zone at the top surface of the laminate.

Push-out is the delamination mechanism caused by the thrust force of the drill that is normal to the plane of ply and occurring when the drilling tool approaches the exit plane where the tool exits the workpiece, the thickness of the uncut material beneath the cutting tool is reduced which leads to a decrease in the rigidity or stiffness of the uncut plies. This will lead to large displacements of the uncut plies beneath the cutting tool that consequently leads to the initiation of delamination. Fig. 2.1(b) shows a schematic diagram of drilling operation with a push-out delamination occurring at a particular uncut thickness. It is a common practice in the industry to avoid the problem of delamination by applying a peel-off (or back-up) ply at the tool exit plane.

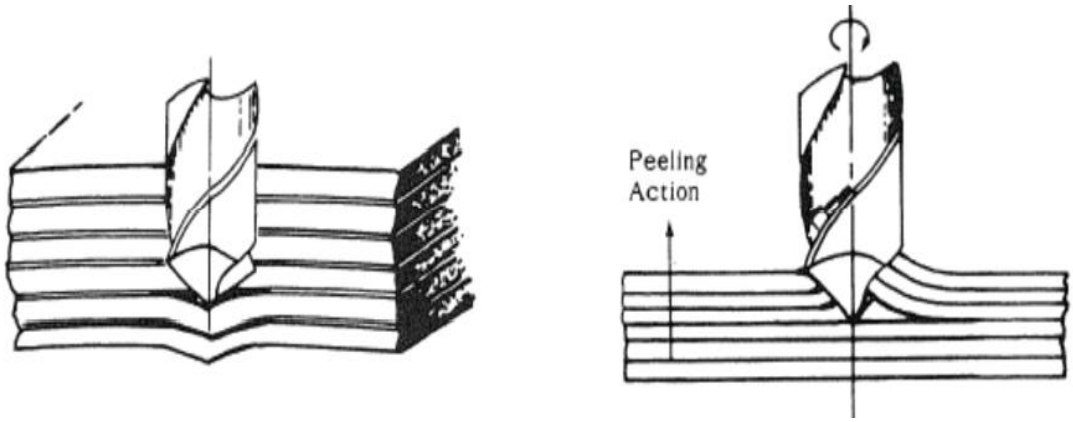

(a) **(b)**

Fig 2.1 shows (a)Push out delamination at exit (b)Peel up delamination at entrance [24]

2.2.2 Matrix Cracking

Matrix cracking is the initial mode of failure and if severe enough will lead to delamination of the plies and eventual failure of the laminate. Although matrix cracking is very localized it can be very difficult to detect. The energy required for matrix cracking is relatively low, for a brittle carbon/epoxy composite.

2.2.3 Fiber Breakage

It is commonly known that at the point of fiber fracture during loading the composite material will generally fail catastrophically. If large enough, local stress concentrations at the tip of a matrix crack are able to initiate cracking of the adjacent reinforcing fibers. Fiber failure is largely dependent on the materials characteristics

and can occur through many types of damage initiation, i.e. transverse impact loading or compression fatigue cycling.

2.2.3 Debonding

It is the process in which under loading the material at the notch tip fractures and a small crack forms in the matrix. Load, once carried by the matrix, is transferred by shear to the fibers which are still intact. These shear forces become so large that the bond between fiber and matrix fails. A cylindrical crack at the interface propagates from the matrix crack surface along the fiber as the applied load increases. The process of debonding is controlled by two parameters: the fiber debond stress, and the rate of increase of stress along the length of debonded fiber due to friction. After the matrix cracks, the fiber stress at the interfacial (debond) crack front is the debond stress. Fig. 2.2 (a) shows a schematic diagram of debonding and fiber pullout.

2.2.4 Fiber pullout

Fiber pullout can be defined as the tearing away of fiber/resin from the wall of the machined edge. It is one of the important energy dissipating fracture processes in fiber reinforced or glass matrix composites. The load transfer between fiber and matrix is still possible by interfacial forces due to matrix shrinkage on to the fiber during manufacture. This friction produces a non-uniform stress along the debonded fiber. Because of the variable strength of the fiber along its length, the fiber is able to break some distance from the matrix crack-plane where the stress is highest. It occurs due to absence of strong chemical bond, lower flexural strength causes easy deformation of hole, which subsequently leads to hole shrinkage, higher tool wear due to abrasion by hard fibers, presence of powdery chip which is a health hazard and is difficult to handle, lower thermal conductivity causing local heat accumulation. Fig. 2.2 (b) shows a schematic diagram of fiber pullout.

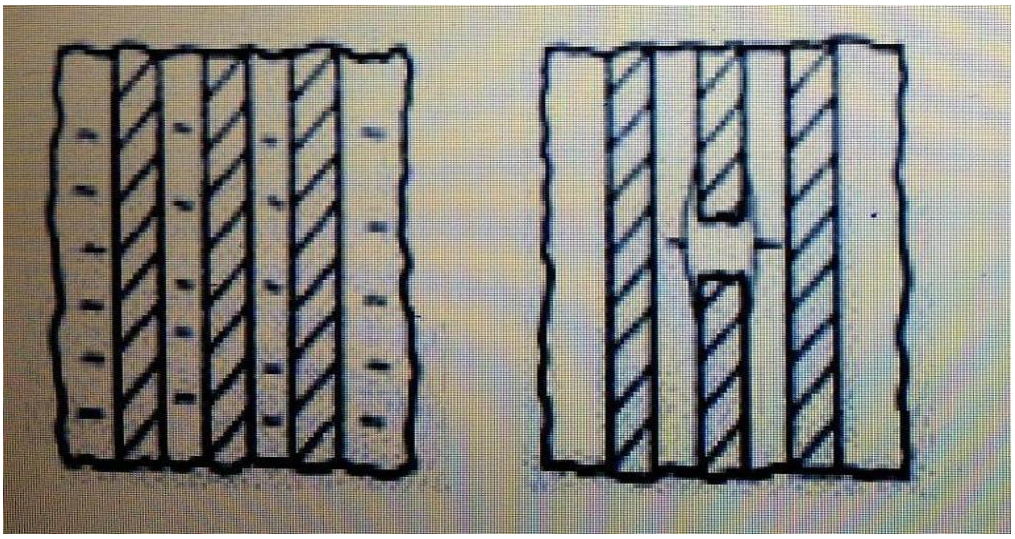

(a) **(b)**

Fig: 2.2 shows (a) Debonding (b) Fiber pullout [25]

2.3 Damage evaluation in composites

2.3.1 Scanning electron microscopy (SEM)

A scanning electron microscope (SEM) is a type of electron microscope that images a sample by scanning it with a focused beam of electrons in a raster scan pattern. The electrons interact with the atoms that make up the sample producing signals that contain information about the sample's surface topography and composition.

Scanning process and Image formation

In a typical SEM, an electron beam is thermionically emitted from an electron gun fitted with a tungsten filament cathode. Tungsten is normally used in thermionic electron guns because it has the highest melting point and lowest vapour pressure of all metals, thereby allowing it to be heated for electron emission, and because of its low cost. The electron beam is focused by one or two condenser lenses to a spot about 0.4 nm to 5 nm in diameter. The beam passes through pairs of scanning coils or pairs of deflector plates in the electron column, typically in the final lens, which deflect the beam in the *x* and *y* axes so that it scans in a raster fashion over a rectangular area of the sample surface. The energy exchange between the electron beam and the sample results in the reflection of high-energy electrons by elastic scattering, emission of secondary electrons by inelastic scattering and the emission of electromagnetic radiation, each of which can be detected by specialized detectors. The beam current

absorbed by the specimen can also be detected and used to create images of the distribution of specimen current. Electronic amplifiers of various types are used to amplify the signals, which are displayed as variations in brightness on a computer monitor (or on a cathode ray tube). Each pixel of computer video memory is synchronised with the position of the beam on the specimen in the microscope, and the resulting image is therefore a distribution map of the intensity of the signal being emitted from the scanned area of the specimen.

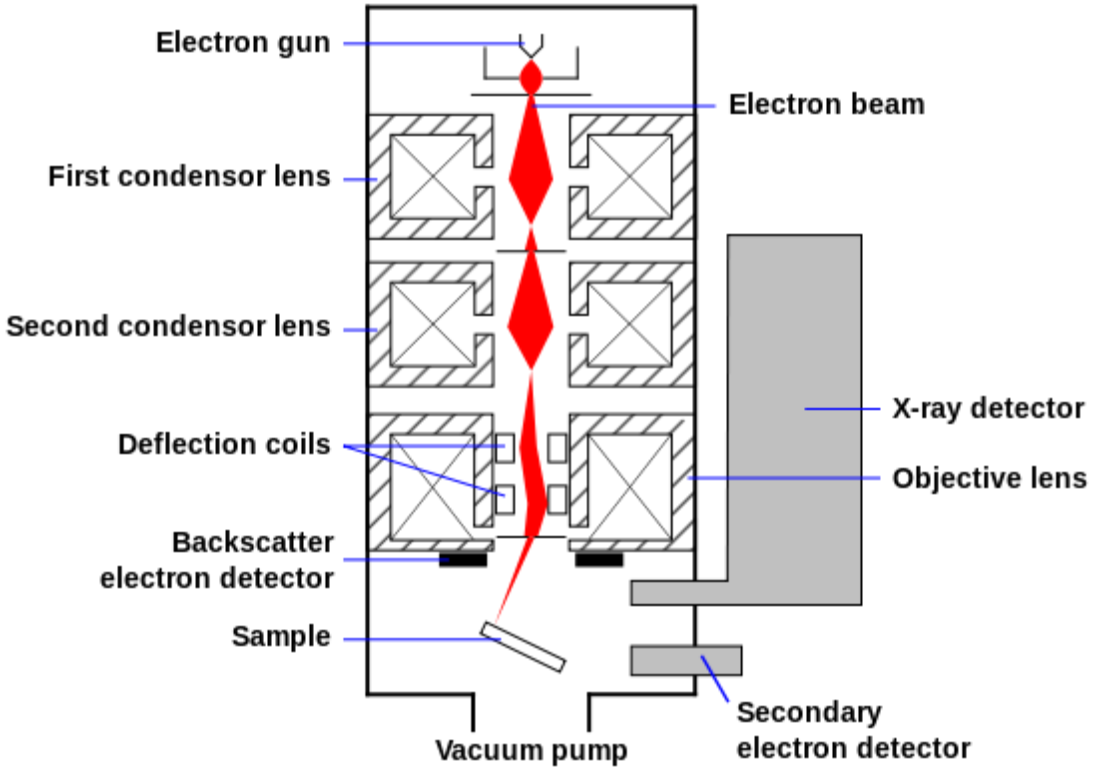

Fig: 2.3 SEM [26]

2.3.2 Optical Microscopy

Optical (light) microscopy involves passing visible light transmitted through or reflected from the sample through a single or multiple lenses to allow a magnified view of the sample. The resulting image can be detected directly by the eye, imaged on a photographic plate or captured digitally.

It has been used for many decades to provide insight into the micro and macrostructure of fiber-reinforced composites. The most widespread use of optical

microscopy for composites is determining void content, ply counts, and fiber orientations. While this makes up the majority of analysis, the investigation of failure mechanisms and micro structural analysis is also common. Furthermore, insight into fiber morphology, matrix modifiers, fillers, and the effect of processing parameters used for manufacturing composite materials are also elucidated using optical microscopy techniques. In some cases, etchants, stains, or dyes may be required for further clarification of the morphology or crack identification. If reflected techniques do not yield the required information, transmitted-light optical microscopy can provide insights into the microstructures of these materials that would otherwise remain hidden when using standard bulk metallographic preparation techniques and reflected illumination. Because many thermoset materials are inert to metallographic etchants, often the sample is best observed with transmitted polarized.

2.3.3 Scanning Technique for Delamination

An accurate inexpensive technique for measuring the delamination size within 10^{-3} mm resolution has been used. The equipment required for this technique are: PC, color flatbed scanner and image software (CorelDraw). The specimen was placed directly on the glass plate of the scanner (it is recommended to put a transparence on the glass plate of the scanner to protect it from the abrasive nature of the polymeric composite materials). The Photo of the drilled specimen was acquired, with 400 dpi, using the software supplied with the scanner or using the CorelDraw software directly. Shadow zone (delamination) was clearly observed around the drilled hole due to the transmitted light through it. Using the contrast, brightness and focusing utilities the shadow zone can easily distinguish from the other undamaged area. The file was saved in JPEG format. This file was imported to the CorelDraw program and the photo was magnified up to 30X. A circle was drawn to the delamination (shadow) zone. The CorelDraw program gives the diameter of the circle within 10-3 mm. The delamination factor, Fd is defined as the quotient between the maximum delaminated diameter, Dmax and the hole nominal diameter, D.

$$F_d = D_{max}/D \qquad \text{(Equation…1.1)}$$

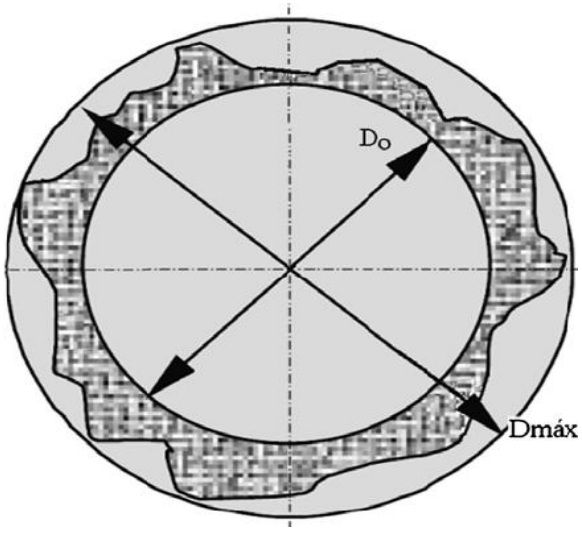

Fig. 2.4 represents measurement of maximum delaminated and hole diameters [27]

CHAPTER 2 LITERATURE REVIEW

An extensive literature review has been carried out for defining the research problem. By adding nanoclay to CFRP has not been addressed so far. A summary of the literature is presented here.

H. Hocheng et al. [1] presented a comprehensive analysis of delamination by use of various drill types: saw drill, candle stick drill, core drill and step drill. In this analysis, the critical thrust force at the onset of delamination for drills was mathematically predicted and compared with the conventional twist drill.

U.A. Khashaba et al. [2] investigated the influence of some parameters on the thrust force, torque and surface roughness in drilling processes of fiber-reinforced composite materials. The parameters considered include cutting speed, feed, drill size and fiber volume fraction. The behavior of thrust force and torque during the drilling cycle was very different. For example at low speed and investigated feeds, the behavior of thrust force and torque as the following: (a) the start point of torque cycle was delayed by a few seconds than the thrust force, (b) at the beginning of the cycles, when chiseling edge contact with workpiece, the thrust force rises quickly, while torque was rapidly increased when the cutting lips start to engage in machining, (c) during the full engagement of the drill the thrust force drops gradually and went to zero. For epoxy resin, increasing cutting speed had insignificant effect on thrust force. The cutting speed and feed had insignificant effect on surface roughness. For GFREC the surface roughness was improved by increasing cutting speed and fiber volume fraction.

H. Hocheng et al. [3] considered delamination the major concern in manufacturing the parts and assembly. The applications of special drill bits, step drilling, pilot hole, back-up plate and various non-traditional machining methods had been reviewed. The special drills show different level of the drilling thrust force varying with the feed rate. A feed rate strategy could avoid delamination caused by the thrust in drilling. The non-traditional drilling methods such as Waterjet, ultrasonic machining, Laser cutting possess were also reviewed.

Antonio T. Marques. [4] investigated the effect of different tool geometries: twist, Brad, Dagger, step drill and cutting parameters: feed, speed on thrust force and delamination during drilling. In order to evaluate damage, enhanced radiography was applied. The resulting images were then computational processed using a previously developed image processing and analysis platform. Results show that the step drill and a correct selection of cutting parameters reduced the thrust force and delamination.

Luis Miguel P. Durao. [5] studied the effect of two variables on the drilling process of composite materials: the tool material and the tool geometry. The two tool materials – tungsten carbide (WC) and polycrystalline diamond (PCD) with the same twist drill geometry were evaluated. The three different tool geometries considered were twist, Brad and step were assessed. The parameters analysed were: thrust force, delamination and mechanical strength through open-hole tensile test, bearing test and flexural test on drilled plates. A proper combination of all the factors involved in drilling operations like tool material, tool geometry and cutting parameters, such as feed rate or cutting speed lead to the reduction of delamination damage and enhancement of the mechanical properties of laminated parts in complex structures, evaluated by open-hole, bearing or flexural tests.

Antonio T. Marques et al. [6] compared four different drills in terms of thrust force during drilling and delamination caused by drilling operation. In order to evaluate delamination damage, enhanced radiography was applied. The resulting images were then processed using a previously developed image analysis and processing platform. Results show that a correct choice of drill geometry, cutting speed or feed rate reduced delamination.

A.M. Abrao et al. [7] presented a review on the drilling operation of glass fibre reinforced plastics (GFRP) and carbon fiber reinforced plastics (CFRP). Attention was focused on tool material and geometry and their effect on the damage caused on thrust force and torque and related parameters (power and specific cutting pressure) together with hole quality, with emphasis on delamination.

C. C. Tsao et al. [8] considered the thrust force and surface roughness, core drill with drill parameters (grit size of diamond, thickness, feed rate and spindle speed) in drilling carbon fiber reinforced plastic (CFRP) laminate. The experimental results indicated that thickness and feed rate are recognized to make the most significant contribution to the overall performance.

C.C. Tsao et al. [9] concluded that the feed rate and spindle speed are the main parameters among the three control factors (diameter ratio, feed rate, and spindle speed) that influence the thrust force and delamination. The effect of diameter ratio was relatively insignificant. A small feed rate was shown to produce low thrust force in drilling, which reduced the extent of induced delamination.

V.N. Gaitonde. [10] studied the effect of process parameters on delamination during high-speed drilling of carbon fiber reinforced plastic (CFRP) composite. The damage caused at the entrance of the drilled hole was characterized by delamination factor, which was evaluated by considering cutting speed, feed rate and point angle. The drilling experiments using cemented carbide (K20) twist drills were performed based on full factorial design of experiments with three levels defined for each of the process parameters. The effects of cutting speed, feed rate and point angle on delamination factor were analyzed using the models by generating response surface plots. The study suggested that delamination tendency decrease with increase in cutting speed and at low values of feed rate and point angle combination.

Luis M. Durao et al. [11] carried out drilling of carbon fibre/epoxy laminates using different cutting parameters and drill geometries was completed for the purpose of this work. The aim was to reduce delamination. Thrust forces during drilling were monitored and delamination measured with the help of enhanced radiography and image processing and analysis computational techniques. The setting of parameters that allowed for thrust force and delamination minimization was a feed rate of 0.025 mm/rev and a cutting speed of 53 m/min. Thrust force reduction was around 12% for feed rate and 35% for cutting speed and delamination reduction potential is around 4-5% when using these combination of cutting parameters.

David Aspinwalla et al. [12] concluded that when drilling, machinability problem especially due to carbon fiber reinforced plastics is inherent anisotropy/in-homogeneity, limited plastic deformation and abrasive characteristics. The paper outlines the experimental results when twist drilling 1.5mm diameter holes in 3mm thick CFRP laminate using tungsten carbide (WC) stepped drills. The control variables considered were prepreg type (3 types) and form (unidirectional (UD) and woven), together with drill feed rate. The longest tool life was achieved when drilling woven MTM44-1/HTS OC at a feed rate of 0.4 mm/rev. Measured thrust forces ranged from 40 to 86N for first hole drilled while for the last hole it was between 64 and 121 N. The results suggest adopting a maximum allowable operating feed rate of 0.2 mm/rev for the stepped drill configuration employed.

I. Singh et al. [13] studied the effect of the cutting speed, the feed rate, and the drill point geometry on the residual tensile strength of the drilled unidirectional glass fiber reinforced epoxy composite using the Taguchi method. The optimum levels of the drill point geometry, the cutting speed and the feed rate had been established for getting maximum residual tensile strength in drilled glass fiber reinforced plastic laminates. The maximum residual strength was found with 8-facet drill at cutting speed of 750 rpm and feed rate of 15 mm/min. It could be concluded that the drilling-induced damage at higher cutting speeds severely affects the residual tensile strength of drilled laminates. The optimum selection of the drill point geometry was also important to ascertain the minimum drilling induced damage and subsequently the maximum residual tensile strength.

P.K. Rakesh et al. [14] presented a generic finite element model in order to investigate to failure of unidirectional glass fiber reinforced plastics (UD-GFRP) composite laminates with drilled hole under uni-axial tensile testing. The initial experimental work done in the field of drilling of GFRP composite laminates and correlated the drilling parameters with the residual tensile strength of composite laminates. The failure of the laminate starts around the hole and polymer matrix fails initially with a cracking sound followed by fiber-matrix debonding. Thereafter, with the increasing time steps, the progressive shear damage takes place around the drilled hole when a uni-axial tensile load was applied.

L.M.P Durao et al. [15] compared two combinations of the drilling process were tool materials-high speed steel (HSS), tungsten carbide (WC) and polycrystalline diamond (PCD) with the same twist drill geometry and three different tool geometries of WC drills – Twist, Brad and Step. The open hole tensile test and bearing test were performed as per ASTM D5766 and D5961. Additionally, statistical techniques, like analysis of variance – ANOVA were applied to evaluate the relative importance of each experimental factor. The parameters considered for analysis include: thrust force, delamination extension open-hole strength and bearing strength. The work showed that a proper combination of the factors involved, like tool material, drill geometry or cutting parameters, could help to reduce the occurrence of delamination.

Luis Miguel P. Durao et al. [16] compared and correlated delamination assessment methods based on radiographic data with mechanical test results (bearing test). unidirectional carbon fibre/epoxy laminates plates were drilled with the objective of comparing the performance of three different tool geometries, combined with three feed rates. One of the drills, twist drill had two distinct materials. Relevant results considered for assessment were the delamination extension by the delamination factor and by the adjusted delamination factor, circularity of the damaged area by the Circularity Index and the mechanical strength by the Bearing stress test. The feed rate influence on damage onset and propagation was well known and the results confirmed that higher feed rates correspond to higher delamination extension. So, feed rates should be kept as conservative as possible, in order to avoid large delamination around the drilled hole. When considering the machining of composite plates, particularly drilling, a good combination of tool geometry combined with an adequate feed rate for the stacking sequence of the plate was essential in order to had worthy results for minimum delamination.

A. Vibhav et al. [17] presented a comparative study of drilling in a carbon fiber reinforced plastic (CFRP) laminate for both conventional and ultrasonically assisted drilling techniques. The effectiveness of ultrasonically assisted drilling (UAD) when compared to conventional drilling (CD) was demonstrated in terms of reduction in the average thrust force. The average thrust force reduction was observed to be as high as 30% under certain drilling conditions.

T.V. Rajamurugan et al. [18] considered the four important input variables for study spindle speed, tool feed rate, drill diameter and fiber orientation angle. The influences of all machining parameters on delamination factor had been analysed based on the developed mathematical model. The developed model was effectively used to predict the delamination in drilling of GFRP composites within the factors and their limits. The result indicated that the increase in feed rate and drill diameter increases the delamination size whereas there was no clear effect observed for fiber orientation angle. The spindle speed showed only little effect on delamination in drilling of GFRP composites.

Luis Miguel P. Durao et al. [19] compared and correlated delamination assessment methods based on radiographic data with mechanical test results (bearing test). Delamination was considered as one of the most critical damages that could decrease in the mechanical strength of the part. The carbon/epoxy plates were drilled with different drills and the resultant delamination extensions were measured from digital enhanced radiographies.

Vijayan Krishnaraj et al. [20] studied an experimental investigation of a full factorial design performed on thin carbon fibre reinforced plastics (CFRP) laminates using K20 carbide drill by varying the drilling parameters such as spindle speed and feed rate to determine optimum cutting conditions. The hole quality parameters analyzed include hole diameter, circularity, peel-up delamination and push-out delamination. Analysis of variance (ANOVA) was carried out for hole quality parameters and their contribution rates were determined. Genetic Algorithm (GA) methodology was used in the multiple objective optimization to find the optimum cutting conditions for defect free drilling. Tool life of the K20 carbide drill was predicted at optimized cutting speed and feed.

DeFu Liu et al. [21] studied the mechanical drilling on composite laminates including the drilling operations (conventional drilling, grinding drilling, vibration-assisted twist drilling and high speed drilling), drill bit geometry (twist drill bit, brad drill bit, step drill bit, straight-flute drill bit, core drill bit) and materials, drilling-induced delamination and thrust force, tool wear approaches to reduce delamination. Feed rate was found to be largest contribution to delamination, thrust force, and tool

wear during drilling of composite laminate. Generally, the use of low feed rate and high cutting speed favored the minimum drilling-induced delamination and extend tool life.

T.J. Grilo et al. [22] studied the influence of three distinct drill geometries, an helicoidal drill with a 140º point angle designated by R415, a four-flute drill designated by R950, and a spur drill designated by spur and cutting parameters, feed rate and spindle speed in the delamination was assessed through delamination factors. A non-destructive method, based on processed images analyses of the drilled surfaces, was used to measure the delaminated area and the maximum diameter of damage zone. The best results were obtained with a spur drill

CHAPTER 3 RESEARCH PROBLEM

3.1 Gaps in literature

From the literature survey, it is found that majority of research work has been done to investigate roughness, defects and their propagation, determination of optimum machining parameters to reduce failure occuring during drilling in composites.

However a study on nanoclay modified epoxy reinforced with carbon fiber laminate has not been performed so far.

3.2 Research Problem

An analysis of process parameters i.e. feed, speed, drill geometry and nanoclay content on residual tensile strength, bearing strength and delamination of carbon fiber reinforced epoxy clay nanocomposites.

3.3 Objectives of the present work

1. Synthesis of Carbon fiber reinforced nanocomposites with matrix modified with different concentrations of nanoclay (0.5%, 2%, 3%).
2. Optimization and modelling of process parameters involved in drilling of fiber reinforced plastic.

CHAPTER 4 EXPERIMENTATION

4.1 Introduction

This chapter includes details regarding the size and specifications of various specimens, their fabrication procedure and the experimental setup required to carry out proposed work.

4.2 Materials

Unidirectional Carbon fiber mat was purchased from BASF Construction Chemicals (India) Private Limited. The Matrix, Araldite CY-230 epoxy and Hardener-951 was purchased from Huntsman India limited. Cloisite 30B®, Organically modified nanoclay was purchased from Southern clay products.

4.3 Specimen Specifications

Carbon fiber mat had been used for making specimen. The 8 carbon sheets used for making composite laminates and final thickness of 4mm were produced. Then the specimens had been cut from the laminates and prepared for mechanical tests carried out were the Open hole tensile and bearing tests as per ASTM standards D5766 and ASTM D5961 respectively. The dimensions of specimens are shown below.

Table 4.1 Specimen Specifications for Testing

Parameters for Specimen	**Specimens for Open hole Tensile Testing**	**Specimens for Bearing Testing**
Length	250 mm	138 mm
Width	36 mm	38 mm
Thickness	4 mm	4 mm
Hole Distance	centrally located hole i.e 125 mm	distance from the edge to hole centre, 20 mm

4.3.1. Specimen Dimensions

1. **For tensile test**

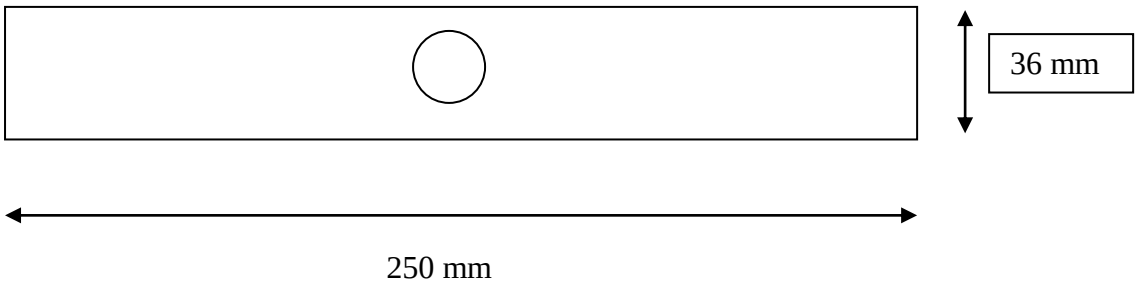

Fig: 4.1 Specimen dimensions for tensile test

2. **For bearing test**

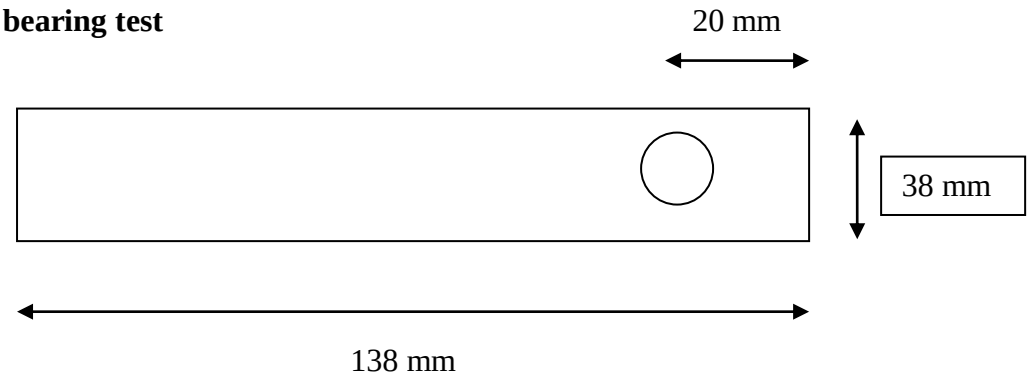

Fig: 4.2 Specimen dimensions for bearing test

4.3.2 Cutting of carbon fiber sheet

For the experimentation unidirectional roll of carbon fiber was purchased having 30 cm width woven with polymer fibers. The sheets were initially cut from roll in length of 300 mm and 150 mm.

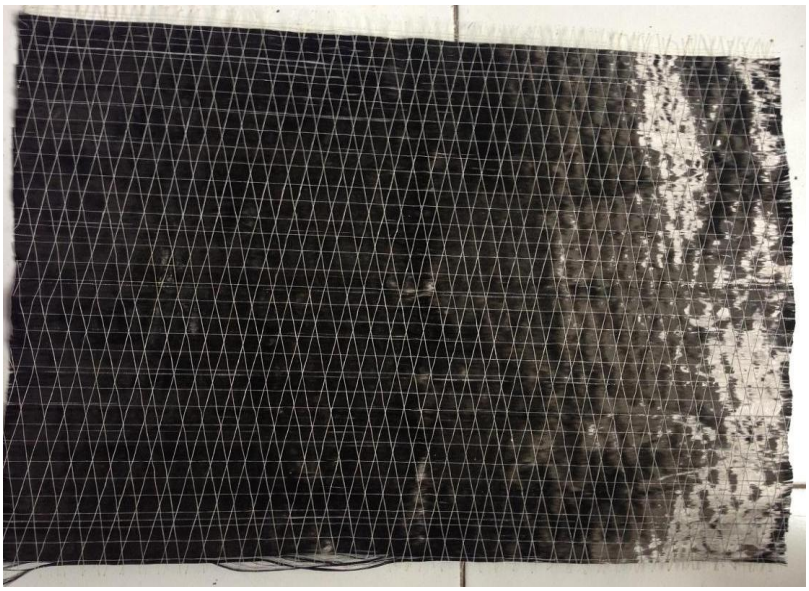

Fig 4.3 Uncoated carbon fiber mat for making specimen

4.4 Synthesis of fiber reinforced nanocomposites:

The fiber reinforced nanocomposites were prepared by dispersing the nanoclay into epoxy resin, addition of hardener in stochiometric quantity and finally application of modified epoxy on carbon fiber mat by hand layup method. Eight layer laminate having 4mm thickness were prepared and finally cut to required sizes after curing of matrix.

4.4.1 Apparatus and equipment used

1. Borosilicate beakers of 10 ml, 250 ml and 500 ml capacity.
2. Electronic weight Machine having capacity of 600 gm.
3. Mechanical stirrer with a maximum RPM of 3000.
4. Water bath sonicator for the sonicaton of nano-composites.

4.4.2 Mixing of Nanoclay into Epoxy (base):

Mechanical stirring: Epoxy base is a transparent in colour thick fluid. It is quite difficult to mix nano particles into it manually. A remi stirrer and an oil bath is used for dispersing nanoclay in epoxy resin. Oil bath was used to heat up the epoxy to desired (80°C) temperature. At this temperature the resin viscosity is reduced, which helps in uniform dispersion of nanoclay in epoxy. Different weight percentages of

nanoclay i.e. 0.5, 2 and 3 wt% by weight of epoxy, were added and stirred at a temperature of 80°C for 1 hour.

Fig: 4.4 Oil bath set-up with mechanical stirrer [Fluid Particle Mechanics Lab, Thapar University, Patiala]

Ultrasonic mixing: Sonication is the process in which the sound energy is applied to agitate particles in a sample, for various purposes. In the laboratory, it is usually carried out using an ultrasonic bath or an ultrasonic probe, known as a sonicator. Sonication is used to speed dissolution, breaking intermolecular interactions, increasing the spacing between interlayers of nanoclay, which is necessary for intercalation of epoxy into nanoclay galleries. It is also done for evenly dispersing nanoparticles into liquids.

Fig: 4.5 Ultrasonication bath [Fluid Particle Mechanics Lab, Thapar University, Patiala]

4.4.3 Mixing of Epoxy Base Solution with Hardener

After ultrasonication, the hardener is added in a ratio 10:1 by weight. While stirring the modified epoxy for 10 to 15 minutes.

4.4.4 Coating of nanoclay mixed epoxy to carbon fiber sheets

The mixture was then poured on to the 8 pieces of carbon fiber sheets one by one and applied uniformly using the hand layup method and then placed these sheets on each other to prepared the composite laminates. The weight were distributed on the top of the laminates so they pressed properly. For this a steel scraper was used to maintain uniformity of the applied solution. It was ensured that there were no air bubbles entrapped inside the epoxy applied on sheets otherwise it would create a flaw there. After then, the sheets took 24 hours to dry.

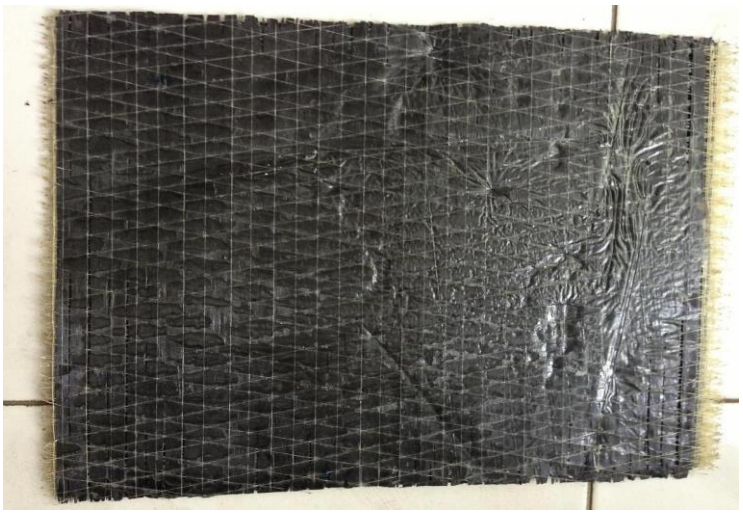

Fig: 4.6 Prepared composite laminate

4.4.5 Curing of the prepared sample

The manufactured laminates were dried in a vaccum oven for 5 hours at 60º C, curing for at least seven days under ambient temperature.

Fig: 4.7 Vaccum Oven [Fluid Particle Mechanics Lab, Thapar University, Patiala]

4.4.6 Cuttnig of sheet for samples

The specimen for tensile test and bearing test were cut as per specifications given in the Table 4.1.

Fig: 4.8 Marble Cutter

4.5 Drilling Operation

Drilling was performed using a radial drilling machine in carbon fiber reinforced Epoxy laminates. Taguchi's method using design of experiments approach had been used to analyze the data collected from experimentation. The Various input parameters had been taken for doing experimentation.

4.6 Experimental Design

In experimental design following points to be concluded:

- Deciding the factors which is to be studied i.e. feed, speed, nanoclay, drill geometry.
- Selecting suitable levels of each factor.
- Selecting proper orthogonal array using Taguchi method and Design of Experiment (DOE).

4.6.1 Various Input Parameters

The various input parameters taken in consideration are feed, speed, nanoclay and drill geometry. Feed rate used in experimentation are coarse and fine. Speed range used are 80 rpm, 445 and 890 rpm. The different nanoclay composition used are 0.5

wt%, 2 wt%, 3 wt%. Three different drill geometries used are step, twist and brad drill.

4.6.2 Output Parameters

The output parameters considered are Residual tensile strength, bearing strength and delamination. The effect of input parameters on these output parameters are studied using ANOVA technique.

4.6.3 Degree of Freedom (DOF)

The number of factors and their interactions and level for factors determine the total degree of freedom required for the entire experiment. The degree of freedom for each factor is given by the number of levels minus one.

DOF for each factor : k-1

where k is the number of level for each factor

DOF for interactions between factors: $(k_A\text{-}1) \times (k_B\text{-}1)$

where k_A and k_B is the number of level for factor A and B

4.6.4 Selection of Factors

The determination of factors which needs to be investigated depends on the responses of interest. There are three (speed, nano-clay, drill geometry) 3-level factors and one (feed) is 2-level factor. The minimum dof required in the experiment are the sum of all the degrees of freedom of factors and their interaction. The number of degree of freedom for factors B, C, D, are two and for factor A is one. As the degree of freedom required for the experiment is 11 the orthogonal array (OA) used for this experimentation is L18 mixed, which have 11 DOF assigned to its various columns. The additional 6 DOF were used to measure the random error. The total degree of freedom for the experiment is explained in Table 4.3. The list of factors with their levels are given in the Table 4.2.

Table 4.2: Factors and their levels of interest

Factors	Level 1	Level 2	Level 3
Feed (mm/rev) (A)	Coarse	Fine	
Speed (rpm), B	80	445	890

Nano-clay content (wt%), C	0.5	2.0	3.0
Drill Geometry, D	Step	Twist	Brad

Table 4.3: Degree of freedom

Factors	**A**	**B**	**C**	**D**	**C × D**	**Total**
Degree of freedom	1	2	2	2	4	11

4.6.5 Selection of Orthogonal Array

Orthogonal Array plays a critical part in achieving the high efficiency of the Taguchi method. The orthogonal array is constructed in a statistically independent manner that each level has an equal no. of occurrences with in each column, and for each level within one column, each level within any other column will occurs an equal number of times as well. Then the columns are called orthogonal to each other. Orthogonal array is available with a variety of factors and levels in the Taguchi method. The selection of orthogonal array will depend on:

- The number of factors and interactions of interest
- The number of levels for the factors of interest

Taguchi orthogonal arrays are experimental designs that usually require only a fraction of the full factorial combinations. To select an appropriate orthogonal array for experiments, the total degrees of freedom must be computed. The number of treatment conditions is equal to the number of rows in the orthogonal array and it must be equal to or greater than the total degrees of freedom.

The most suitable orthogonal array which were used for this experiment is L18. The 18 experimental designs represent the set of values of input process parameters with which particular experiment is to be conducted.

Table 4.4: Experimental L18 Orthogonal Array (Taguchi Design)

Experiment No.	Feed (mm/rev)	Speed (rpm)	Nano-Clay (wt%)	Drill Geometry
1	Coarse	80	0.5	Step
2	Coarse	80	2.0	Twist
3	Coarse	80	3.0	Brad
4	Coarse	445	0.5	Step
5	Coarse	445	2.0	Twist
6	Coarse	445	3.0	Brad
7	Coarse	890	0.5	Twist
8	Coarse	890	2.0	Brad
9	Coarse	890	3.0	Step
10	Fine	80	0.5	Brad
11	Fine	80	2.0	Step
12	Fine	80	3.0	Twist
13	Fine	445	0.5	Twist
14	Fine	445	2.0	Brad
15	Fine	445	3.0	Step
16	Fine	890	0.5	Brad
17	Fine	890	2.0	Step
18	Fine	890	3.0	Twist

4.7 Experimental Procedure

The experiment had been conducted by drilling of carbon fiber composite laminates on radial drilling machine by using three different drill geometry. The tools and machine used for experimentation were explained below:

4.7.1 Tools used in machining

The three different tool geometries of high speed steel such as Twist, Brad, Step drills were used. In experiment these three drill bit of 12 mm diameter had been used for drilling 12 mm diameter hole. Twist drill is a standard drill commonly used. It is

easily available and less expensive. Brad drill has originally designed for cutting of a wood. It has a specific point geometry causing the fiber tensioning prior to cut thus enabling a clean cut of the fibers. The step drill was designed in order to have the small diameter tip as short as possible. This can be a limitation if plates of greater thickness are to be drilled. The specific geometry of the step drill, dividing the drilling operation in two phases, provides a considerable reduction of the maximum thrust force. The Fig 4.9 shows drill geometry of (a)Twist (b) Brad (c) Step.

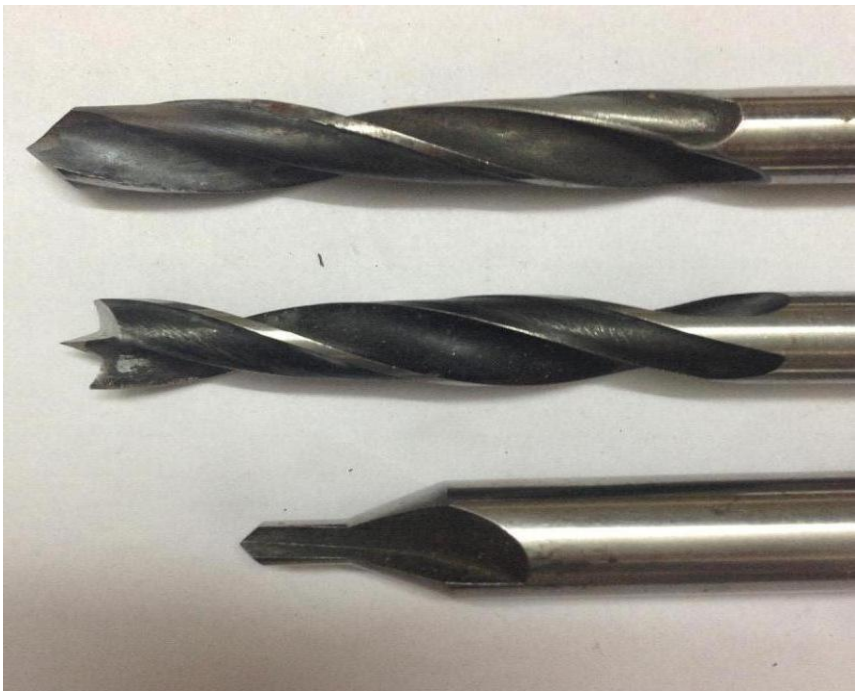

Fig: 4.9 Drill Geometry

4.7.2 Radial Drilling Machine

Radial Drilling machine is a machine fitted with a rotating cutting tool called drill bit. This radial drilling machine is used for drilling holes in various materials such as steel, cast iron, plastics etc. The use of machine is in the metal working industry. A Radial Drilling machine is a large gear headed drill press in which the head moves along the arm that radiates from the column of the machine. The arm of the machine can swing in relation to the base of the machine. This swing operation helps the drill head to move out of the way so a large crane can place the heavy work piece on the base of the machine. Also this helps in drilling holes at different locations of the work piece without actually moving the work piece. Power feed of the spindle is a common feature. It is used for all functions such as drilling, counter boring, spot facing,

lapping, tapping, reaming and boring. Drilling machine holds a certain diameter of drill (called a chuck) rotates at a specified rpm (revolutions per minute) allowing the drill to start a hole.

A Radial Drilling machine is a geared drill head that is mounted on a arm assembly that can be moved around to the extent of its arm reach. The most important components are the arm, column, and the drill head. The drill head of the machine can be moved, adjusted in height and rotated aside from its compact design, the radial drill press is capable of positioning its drill head to the work piece through this radial arm mechanism.

Components of radial drilling machine

Here some of the major parts of the radial arm drilling machine explained below:

Column – It is the part of the radial arm drill press which holds the radial arm which can be moved around according to its length.

Arm Raise – It adjust the vertical height of the radial arm along the column.

On/Off Button – It is the switch that activates and deactivates the drill press.

Arm Clamp – It secures the column and arm in place.

Table – Table is the area where the work pieces are fed and worked on.

Base – It is the radial arm drill press part that supports the column and the table.

Spindle – It is the rotated part of the drill press which holds the drill chuck used in holding the cutting tool.

Drill Head – It is the part of the drill press that penetrates through the material or work piece and drill through the specific hole size.

Radial Arm – It holds and supports the drill head assembly and can be moved around on the extent of its length.

4.8 Experimental Set up

A Radial drilling machine as shown in Fig 4.10 (a) was used for experimental work for drilling holes available at Thapar University, Patiala in the Machine tool Lab. Three different drills were used i.e. Twist, Brad, Step. In experiment drill bits of 12mm were used for drilling holes. Many input parameters like feed, speed, nano-clay, drill geometry varied in this experiment. A radial drilling machine was different range of feed and speed. The different range of speed can be chosen in machine by shifting the gears according to required speed. The drilling of the composite laminate

was shown in the Fig 4.10 (b). All the experiments were performed according to the given design of Taguchi design in table 4.4.

Table 4.5: Speed range of radial drilling machine

Speed (rpm)			
160	244	580	890
80	122	290	445

Different range of feed like coarse and fine can be chosen from the machine. The feed range for coarse was 0.2 mm/rev and for fine was 0.1 mm/rev.

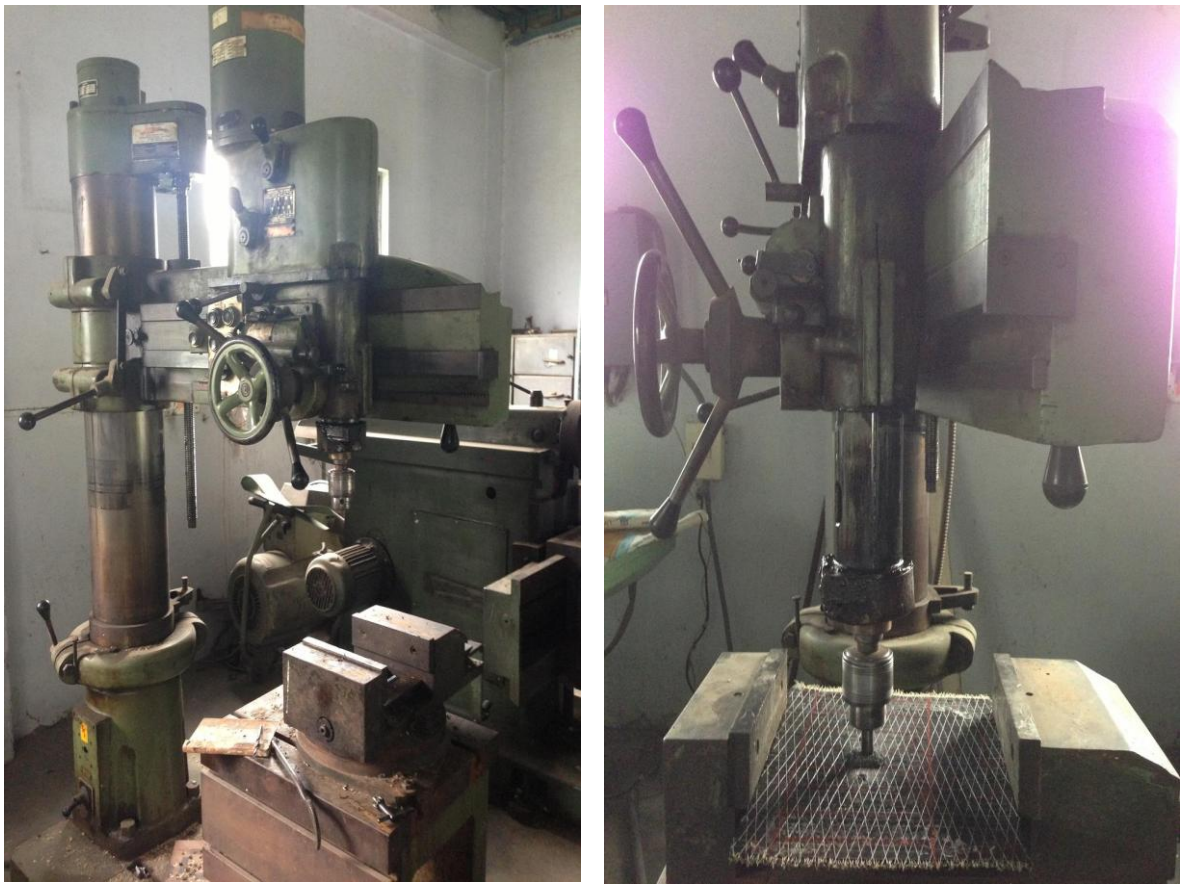

(a) **(b)**

Fig: 4.10 (a) A radial drilling machine (b) Dilling of composite laminate [Machine Tool lab, Thapar University, Patiala]

4.9 Mechanical testing

Mechanical tests performed were the Open-hole tensile test and the Bearing test. These tests were considered with the purpose of assessing the effect of delamination on the mechanical properties of the drilled specimens.

4.9.1 Open-hole Tensile Test

A Universal testing machine (UTM) shown in Fig.4.11 was used for the testing of the carbon fiber reinforced composite specimens for its tensile strength. Maximum Capacity of UTM is 1000 KN. Tensile testing of specimens was performed as per ASTM D5766. This is a computer controlled machine having hydraulic grippers for holding the specimen. This machine is capable of performing both tensile as well as compression tests. The total 36 specimens were tested i.e.12 specimens for each composition. Both the ends of the specimen were held in the grippers of the machine. The Specimens were tested until they break indicating the various parameters like peak load, ultimate stress etc. The specimen before the tensile test and specimen after the test is shown in Fig 4.12. (a), (b)

Fig: 4.11 Universal Testing machine [Structure Lab, Thapar University, Patiala]

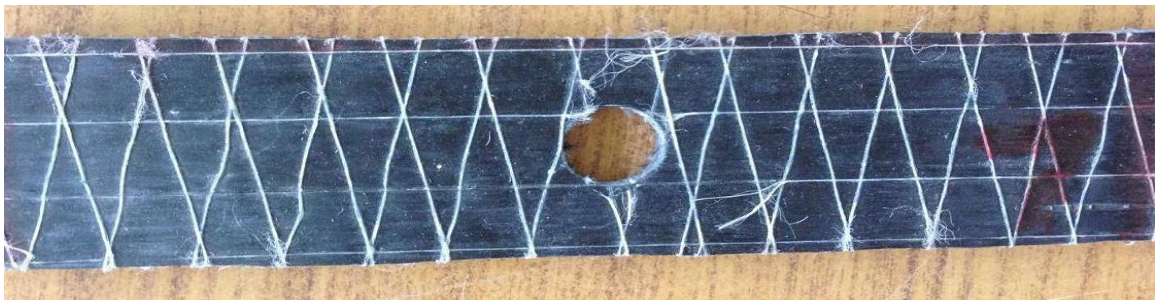

(a)

Fig: 4.12 Specimen before Tensile testing

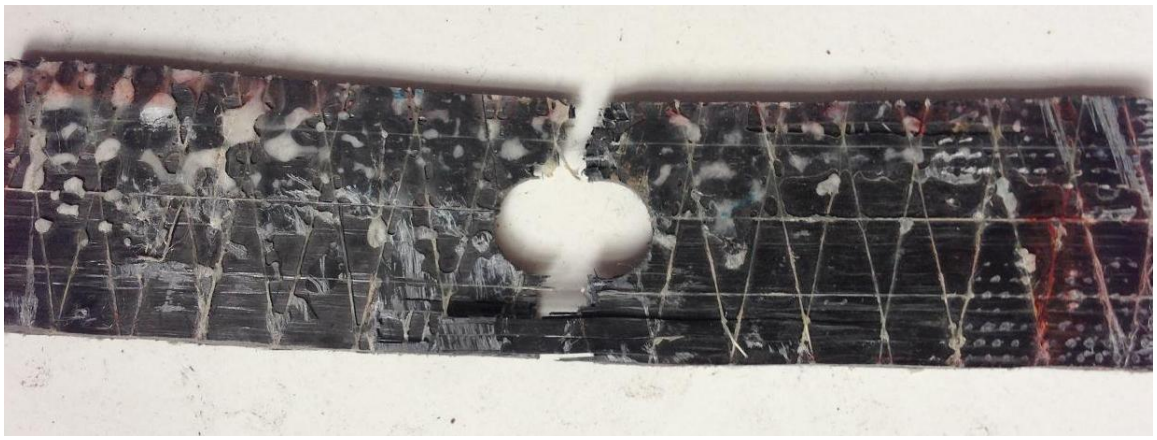

(b)

Specimen after testing

4.9.2 Bearing Test

The testing of specimen was performed as per ASTM D5961. The test fixture made for bearing test was shown in Fig 4.13. It was used to mount the test specimen relative to machine grips. The bearing strength was calculated as the maximum bearing load divided by the product of specimen thickness and hole diameter. The specimen was constrained between the fixture hole with the bolt and the other end of specimen was hold in the machine grip. The specimen before bearing test and specimen after the test was shown in Fig 4.14 (a), (b).

Fig: 4.13 Prepared fixture arrangement for Bearing Test

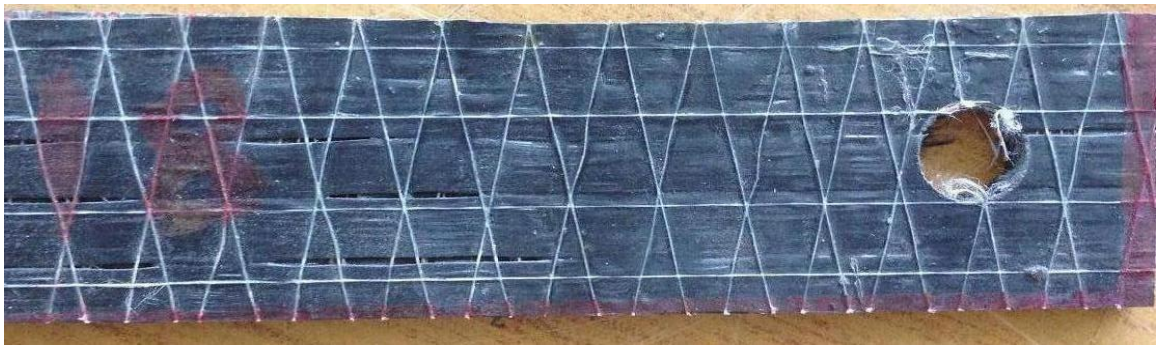

Fig: 4.14 (a) Specimen before testing

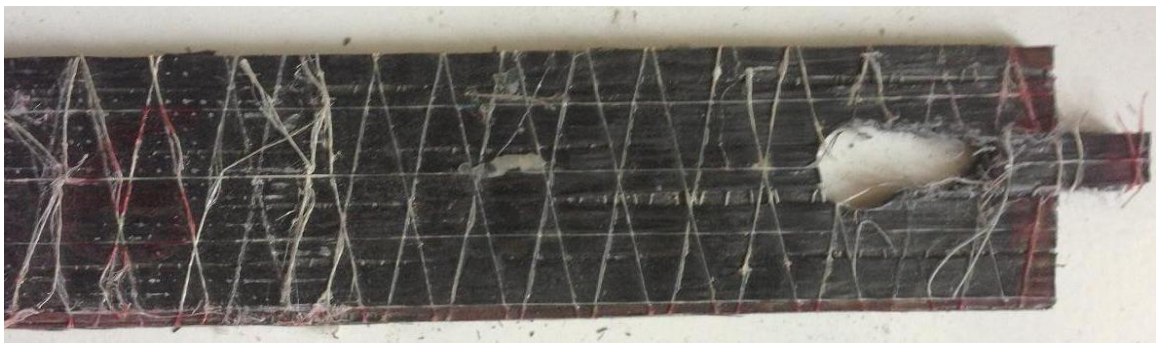

(b) Specimen after testing

4.9.3 Mesurement of Delamination

After the drilling process, it was necessary to evaluate the delaminated region around the drilled hole. This was achieved by using scanning technique [28]. The equipment required for this technique are: PC, color flatbed scanner and image software (CorelDraw). The specimen was placed directly on the glass plate of the scanner (it is recommended to put a transparence on the glass plate of the scanner to protect it from the abrasive nature of the polymeric composite materials). The scanner used was Brother MFC 295 CN. The drilled holes were scanned at a resolution of 1200 dpi and saved as a bitmap image. Shadow zone (delamination) was clearly observed around the drilled hole due to the transmitted light through it. Using the contrast, brightness and focusing utilities the shadow zone can easily distinguish from the other undamaged area. This file was imported to the CorelDraw program and a circle was drawn to the delamination (shadow) zone. The delamination factor, Fd is defined as he quotient between the maximum delaminated diameter, Dmax and the hole nominal diameter, D.

$F_d = D_{max}/D$ (Equation…4.1)

The delaminated zone appears in white whereas the undamaged area remains black as shown in Fig. 4.15. The delamination caused by the three different drill geometries i.e. Step, Twist and Brad drill was shown in fig 4.15.

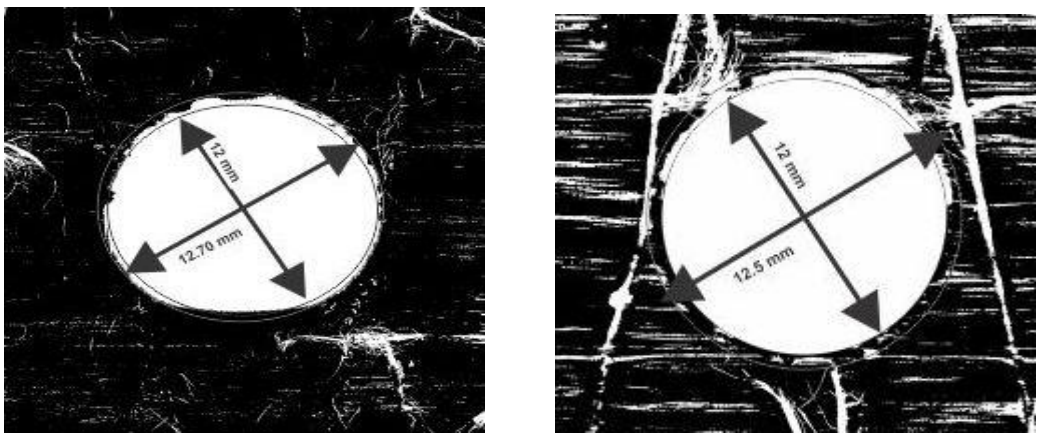

(a) **(b)**

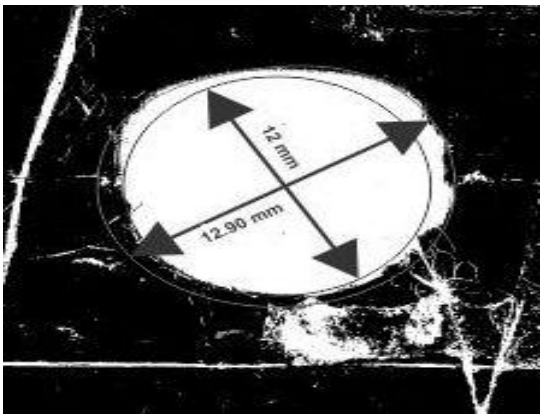

(c)

Fig: 4.15 Delamination caused due to (a) step drill (b) twist drill (c) brad drill

4.9.4 Micro hardness Tester

Micro hardness test as shown in Fig.4.16 was conducted on specimen with different clay loadings to see the effect of clay loading on hardness values. Micro hardness tests were conducted on the computer interfaced micro hardness tester manufactured by Metatech industries, Pune, India.

Fig: 4.16 Micro hardness equipment [Meterology Lab, Thapar University, Patiala]

The load applied was 100gm and the dwell time used during load application was 20 seconds. Micro hardness measured is dependent on the diameter of indentation on the

samples. The indentations were measured by the Quantimet software. The indents formed by pyramid shaped indenter were measured with the help of software and shown in Fig. 4.17. There are two eyepieces available in the instrument of 10X and 40X. Eyepiece of 40X was used for the experiments. The diameter of indent is measured with the software, which gives the direct number for micro hardness.

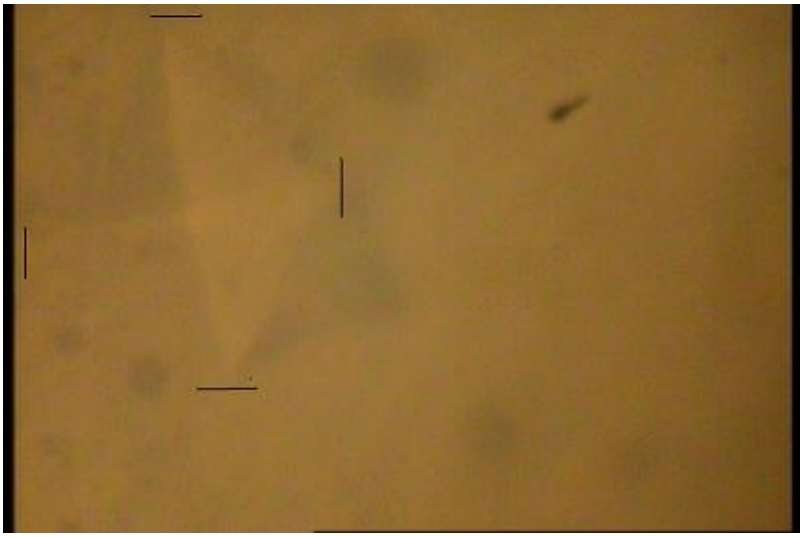

Fig: 4.17 Indent of specimen

4.10 Analysis of results

Signal-to-noise ratio

The parameters that influence the output can be categorized into two classes, namely controllable (or design) factors and uncontrollable (or noise) factors. Controllable factors are those factors whose values can be set and easily adjusted by the designer. Uncontrollable factors are the sources of variation often associated with operational environment. The change in quality characteristic of a product under investigation in response to a factor introduced in the experimental design is the 'signal' of the desired effect. The effect of the external factors (uncontrollable factors) on the outcome of quality characteristic is termed as 'noise'. The objective of any experiment is to achieve the best possible S/N ratio. The best settings of control factors as they influence the output parameters are determined through experiments. From the analysis point of view, there are three possible categories of the response characteristics explained below.

r is the number of tests in a trial (noise of repetitions regardless of noise levels)

$\sum_{i=1}^{r} (y_i)^2$ =Summation of all response values under each trial

(Equation... 4.1)

MSD = Mean square deviation

Y_i = Observed value of the response characteristic

Y_0 = nominal or target value of the results

The three different response characteristics are given by the following.

- Higher the better
- Lower the better
- Nominal the best

1) Higher is better. The S/N for higher the better is given by:

$(S/N)_{HB} = -10 \log (MSD_{HB})$

Where $MSD_{HB} = \frac{1}{r}\sum_{j=1}^{r}(\frac{1}{y_j})^2$ (Equation.. 4.2)

MSD_{HB} = Mean Square Deviation for higher-the-better response.

2) Nominal is better. The S/N for nominal is better is:

$(S/N)_{NB} = -10 \log (MSD_{NB})$

Where $MSD_{NB} = \frac{1}{r}\sum_{j=1}^{r}(y_j - y_0)^2$ (Equation.. 4.3)

3) Lower is better. In this design situation, response is the type of ‘‘lower is better’’, which is a logarithmic function based on the mean square deviation (MSD), given by

$(S/N)_{LB} = -10 \log (MSD) = -10 \log \left[\frac{1}{r}\sum_{i=1}^{r}(y_i)^2\right]$ (Equation.. 4.4)

Where $MSD_{LB} = \frac{1}{r}\sum_{j=1}^{r}(y_j)^2$ (Equation.. 4.5)

Signal to noise ratio for response characteristics

The parameters that influence the output can be categorized in two categories, controllable factors and uncontrollable factors. The control factors that may contribute to reduced variation can be quickly identified by looking at the amount of variation present in response. The uncontrollable factors are the sources of variation often associated with operational environment. For this experimental work, response characteristics have given in the Table 4.6.

Table: 4.6 Response Characteristics

Response Name	Response Type
Bearing strength	Higher the better
Tensile Strength	Higher the better
Delamination Factor	Lower the better

Analysis of variance

The knowledge of the contribution of individual factors is critically important for control of the final response. The analysis of variance (ANOVA) is a common statistical technique to determine the percent contribution of each factor for results of experiment. It calculates parameters known as sum of squares (SS), degree of freedom (DOF), variance, F-ratio and percentage of each factor. Since the procedure of ANOVA is a very complicated and employs a considerable of statistical formulae, only brief description of is given as following.

The Sum of Squares (SS) is a measure of the deviation of the experimental data from the mean value of the data.

Let A be the first factor

$$SS_T = \sum_{i=1}^{r} (y_i - \bar{\bar{T}})^2 \qquad \text{(Equation... 4.6)}$$

Where r = Number of response observations, T is the mean of all observations, y_i is the ith response

Factor Sum of Squares (SS_A) - Squared deviations of factor (A) averages from overall average

$$SS_A = [\sum_{i=1}^{k_A} (\frac{\bar{\bar{A_i}}^2}{n_{Ai}})^1] - \frac{T^2}{N} \qquad \text{(Equation... 4.7)}$$

Where

A_i =Average of all observations under A_i level = A_i/n_{Ai}

T = sum of all observations

$\bar{\bar{T}}$ = Average of all observations= T/N

n_{Ai} =Number of observations under A_i level

Error Sum of Squares (SS_e) - Squared deviations of observations from factor (A) Averages

$$SS_e = \sum_{j=1}^{k_A} \sum_{i=1}^{n_{Ai}} (y_i - \overline{A}_j)^2 \qquad \text{(Equation… 4.8)}$$

where SS_T = Total sum of squared deviations about the mean.

$$SS_{A\times B} = [\sum_{i=1}^{c} (A\times B)_i^2 / n_{(A\times B)i}] - T^2/N - SS_A - SS_B \qquad \text{(Equation… 4.9)}$$

In the ANOVA table mean square deviation is defined as:

MS = Mean Square

$$\textbf{MS} = \frac{\textbf{SS (Sum of squared division)}}{\textbf{DF (Degree of Freedom)}} \qquad \text{(Equation… 4.10)}$$

Measurement of F-value of Fisher's F ratio

The principle of the F test is that the larger the F value for a particular parameter, the greater the effect on the performance characteristic due to the change in that process parameter. F value is defined as:

$$\textbf{F} = \frac{\textbf{MS for a term}}{\textbf{MS for the error term}} \qquad \text{(Equation… 4.11)}$$

5.1 Introduction

The effects of parameters i.e. feed, speed, nanoclay, drill geometry and interaction between nanoclay and drill geometry were evaluated using ANOVA and factorial design. A confidence interval of 95% has been used for the analysis. One repetition for each of 18 trails was completed to measure the Signal to Noise ratio (S/N Ratio).

5.2 Results for Micro-Hardness

The micro-hardness of specimen manufactured at different nanoclay loading was measured. Table 5.1 shows the experimental observations of the nanocomposites with different nanoclay contents. An average hardness was calculated by taking measurements at 3 different points in each specimen.

Table 5.1: Micro Hardness values for different nanoclay loading specimens

Loading points	Micro hardness values for nanoclay loading		
	0.5 wt%	**2 wt%**	**3 wt%**
Point 1	9.181	10.654	10.100
Point 2	9.298	11.159	9.377
Point 3	9.759	11.425	9.756
Average	9.412	11.079	9.744

The maximum hardness has been measured in specimen having 2wt% nanoclay content. A decrease in values of hardness was observed on further increasing the nanoclay content. The slight decrease in the hardness from 11.079 HV (2 wt% of nanoclay) to 9.744 HV (3 wt% of nanoclay) was seen. Thus, adding a small amount of nanoclays could potentially enhance hardness of the material.

5.3 Results for Bearing Test

The results for bearing test for each of the 18 treatment conditions with repetition are given in Table 5.2.

$$\text{Bearing Strength} = \frac{Peak\ Load}{Projected\ area\ of\ the\ hole} \qquad \text{(Equation....5.1)}$$

Where projected area of the hole = diameter of hole × thickness of specimen

d = diameter of hole (mm), t = thickness of specimen (mm)

Table 5.2: Results of specimen for Bearing test

Experiment No	Feed (mm/rev)	Speed (rpm)	Nanoclay (wt%)	Drill Geometry	Bearing test Strength (N/mm^2)		Mean	S/N Ratio
					1	2		
1	Coarse	80	0.5	Step	70.26	60	65.13	36.19
2	Coarse	80	2.0	Twist	140.5	104.4	122.45	41.47
3	Coarse	80	3.0	Brad	80	57	68.52	36.34
4	Coarse	445	0.5	Step	46.30	58.52	52.41	34.21
5	Coarse	445	2.0	Twist	102.66	115.20	108.93	40.69
6	Coarse	445	3.0	Brad	75.16	66	70.58	36.91
7	Coarse	890	0.5	Twist	70	87.27	78.66	37.75
8	Coarse	890	2.0	Brad	110.20	90.14	100.17	39.88
9	Coarse	890	3.0	Step	80.5	97.4	88.95	38.86
10	Fine	80	0.5	Brad	60.42	76.50	68.46	36.52
11	Fine	80	2.0	Step	130.10	91.62	110.86	40.50
12	Fine	80	3.0	Twist	115.50	97.24	106.37	40.44
13	Fine	445	0.5	Twist	89.5	70.6	80	37.88
14	Fine	445	2.0	Brad	111	100.2	105.56	40.43
15	Fine	445	3.0	Step	70.4	102.46	86.43	38.28
16	Fine	890	0.5	Brad	46.41	65.25	55.83	34.56
17	Fine	890	2.0	Step	130.15	100.17	115.16	41
18	Fine	890	3.0	Twist	84	83.8	83.90	38.47

5.3.1 Analysis of Variance – Bearing test

The results for bearing test were analyzed using ANOVA for identifying the significant factors affecting the performance measures. The Analysis of Variance (ANOVA) for the mean bearing test at 95% confidence interval is given in Table 5.3. The various data for each factor and their interaction was p value to find significance of each. The principal of the p value is that the value less than 0.05 then that factors or interactions are significant if value is more than 0.05 then that factors or interactions are insignificant. From the ANOVA Table 5.3 it is seen nanoclay p value is 0.00, drill geometry p value is 0.005 less than 0.05 which means these factors are significant, same speed and feed has p value more than 0.05 so these factors are insignificant. Interaction between nanoclay and drill geometry (C×D) p value is 0.296 more than 0.05 so these factors are insignificant. In the Table 5.4 shows the ranks of various factors in terms their relative significance. 1st rank is given to the nano-clay which means nano-clay has the highest contribution to bearing strength. 2nd rank is given to the type of drill geometry, 3rd rank is given to the feed and the 4th rank is given to the speed that mean speed have the minimum contribution to the bearing strength.

Table 5.3: Analysis of Variance for Means of Bearing Test

Source	DOF	Seq SS	Adj MS	F	P	% Contribution	Status
Feed (A)	1	179.5	179.49	3.18	0.105	2.32	Insignificant
Speed (B)	2	119.1	59.57	1.05	0.384	1.54	Insignificant
Nanoclay (C)	2	5829.9	2914.97	51.61	0.000	75.43	Significant
Drill Geometry (D)	2	1034.7	517.33	9.16	0.005	13.38	Significant
C × D	2	288.3	72.08	1.57	0.296	--	Insignificant
Residual Error	8	276.8	46.48	--	--	--	--
Total	17	7728	--	--	--	100	--

Table 5.4 Response Table for Means of Bearing Strength

Level	Feed	Speed	Nanoclay	Drill Geometry

1	83.98	90.31	66.76	86.50
2	90.30	84.00	110.53	96.73
3	--	87.11	84.13	78.19
Delta	6.32	6.30	43.77	18.54
Rank	3	4	1	2

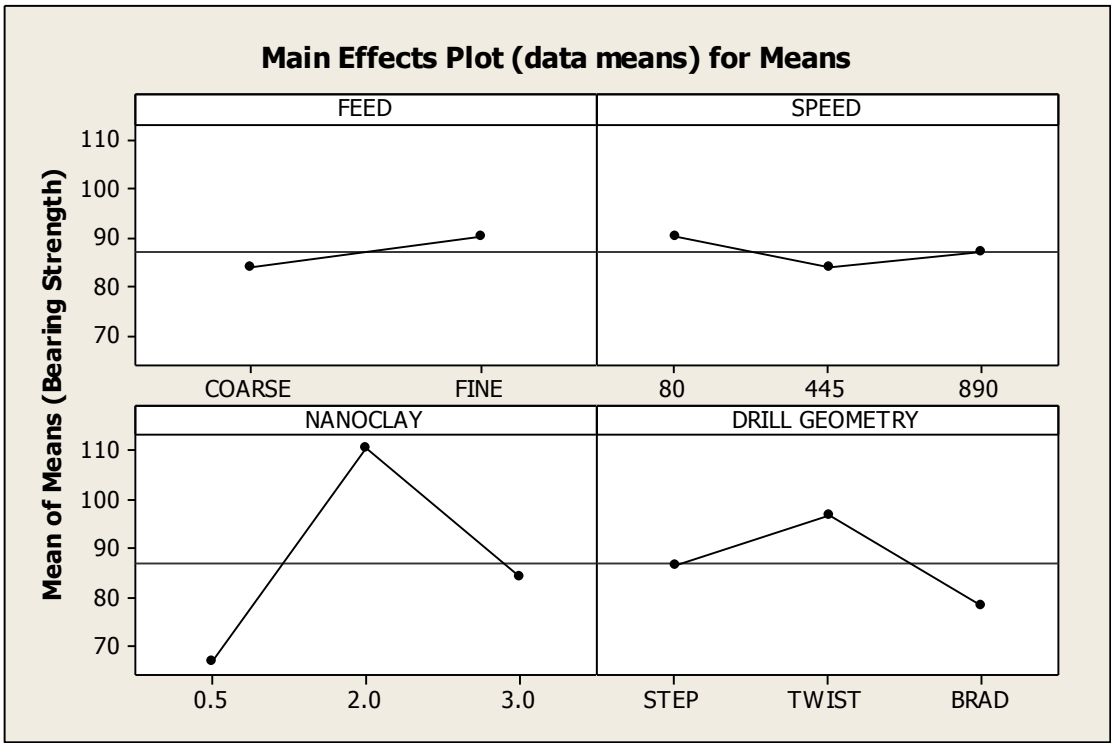

Fig: 5.1 Main effects plot of Bearing Strength for Means

In Figure 5.1 bearing strength is more at feed rate of fine as compare to feed coarse. There are three speed used i.e 80, 445 and 890 rpm the effective one is 80 rpm. Bearing strength increases with increase in nanoclay from 0.5 wt% to 2 wt%. Nanoclay having 0.5 wt% shows the minimum value of bearing strength, 2 wt% nanoclay give highest value of bearing strength and 3 wt% nanoclay give less bearing strength. Similarly step drill give less bearing strength, twist drill give maximum bearing strength and the brad drill has minimum bearing strength. Figure 5.2 shows interaction between nanoclay and drill geometry.

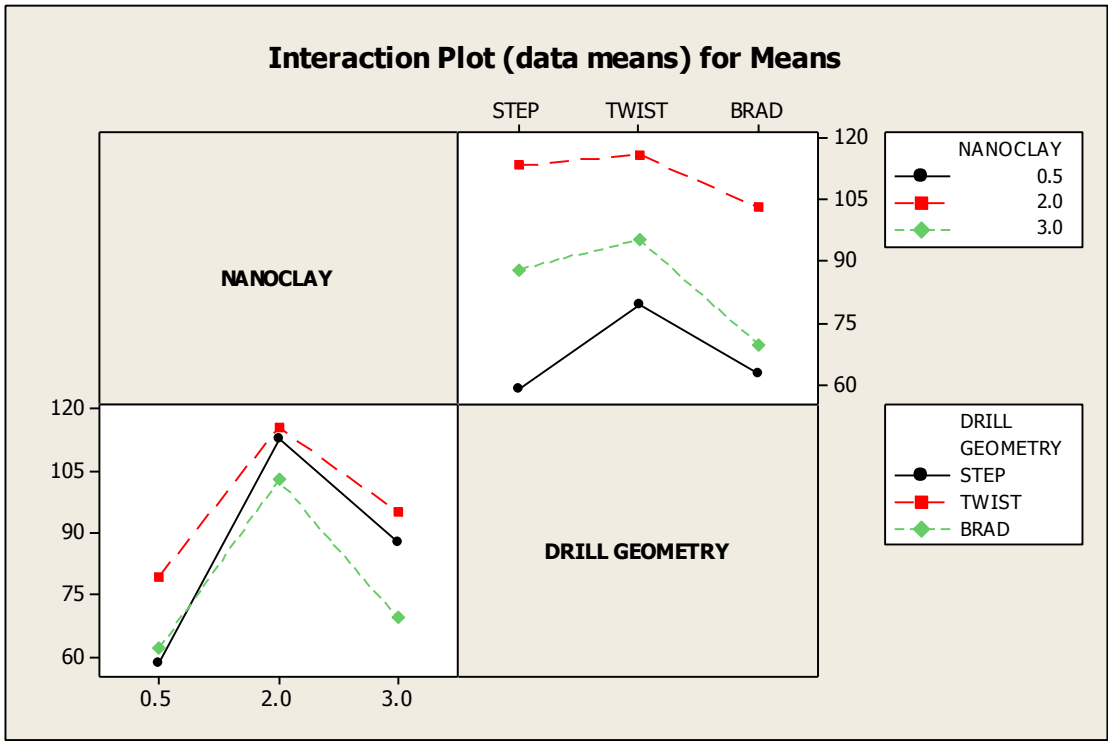

Fig: 5.2 Interaction plot of Bearing Strength

5.3.2 Results for S/N ratio of Bearing test

The S/N ratio consolidates several repetitions into one value and is an indication of the amount of variation present. The S/N ratios have been calculated to identify the major contributing factors and interactions that cause variation in the bearing test. Bearing test is "Higher is better" type response.

Table 5.5 shows the ANOVA results for S/N ratio of bearing test at 95% confidence interval. Nanoclay, drill geometry p values are less than 0.05 so these are significant and feed, speed are insignificant factors having more p value. The interaction between nanoclay and drill geometry is insignificant. Table 5.6 show the ranks for different factors. Main effect plot and interaction plot of S/N ratios for bearing test are shown in the Figure 5.3 and 5.4 respectively.

Table 5.5 Analysis of Variance for S/N ratio of Bearing Strength

Source	DOF	Seq SS	Adj MS	F	P	% Contribution	Status
Feed (A)	1	1.844	1.844	2.05	0.183	2.18	Insignificant
Speed (B)	2	0.8164	0.408	0.45	0.648	0.96	Insignificant

Nanoclay (C)	2	60.298	30.149	33.44	0.000	71.45	Significant
Drill Geometry (D)	2	12.409	6.204	6.88	0.013	14.70	Significant
C × D	4	5.0187	1.257	2.68	0.135	--	Insignificant
Residual Error	6	3.996	0.661	--	--	--	--
Total	17	84.384	--	--	--	100	--

Table 5.6 Response Table for S/N ratio of Bearing Strength

Level	**Feed**	**Speed**	**Nanoclay**	**Drill Geometry**
1	38.04	38.58	36.19	38.18
2	38.68	38.07	40.67	39.46
3	--	38.43	38.22	37.45
Delta	0.64	0.51	4.48	2.01
Rank	3	4	1	2

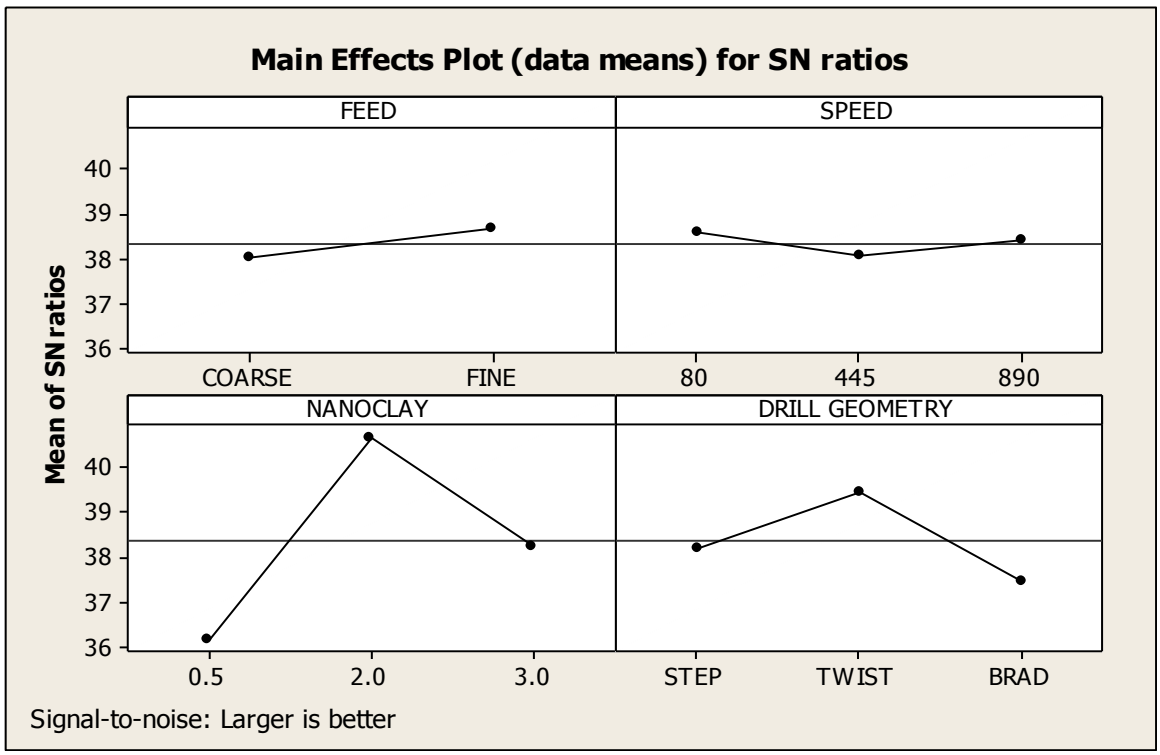

Fig: 5.3 Main effects plot for Bearing Strength of S/N ratio

In Figure 5.3 bearing strength is more at fine feed range as compare to feed coarse. There are three speed range of 80, 445, 890 rpm. Bearing strength increases with increase in nanoclay from 0.5 wt % to 2 wt%. At nanoclay having 0.5 wt% minimum value of bearing strength was observed, 2 wt% nanoclay give highest value of bearing strength and 3 wt% nanoclay give less bearing strength. Similarly step drill give less bearing strength, twist drill give maximum bearing strength and the brad drill has minimum bearing strength.

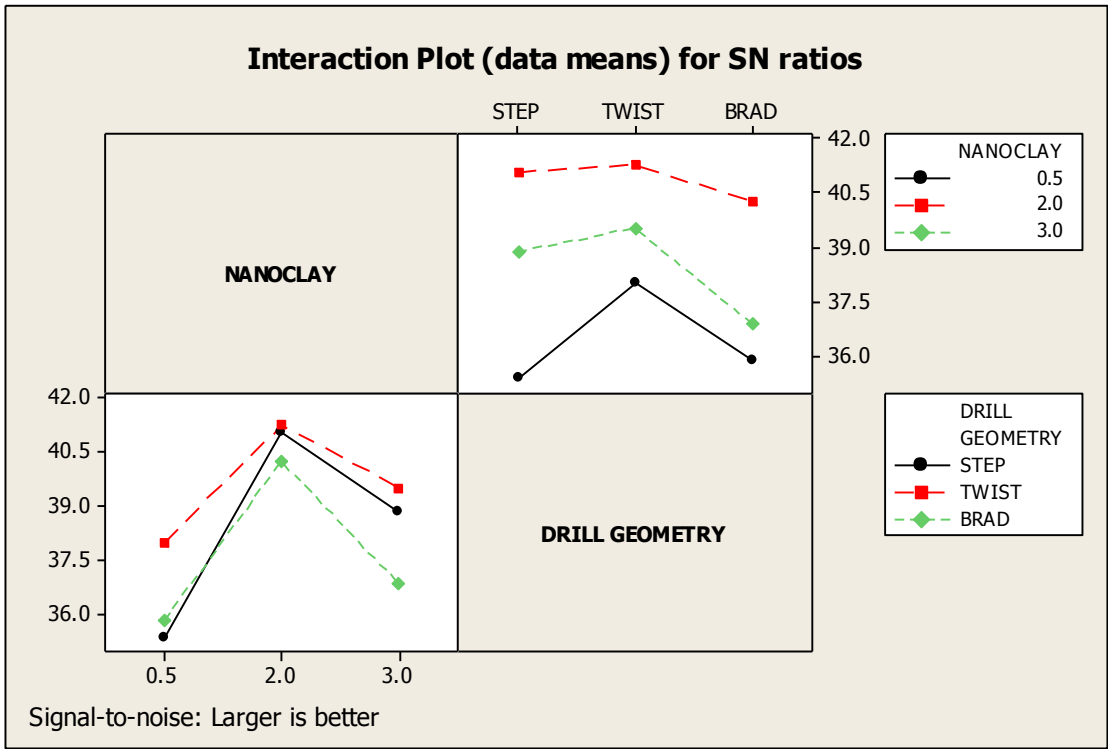

Fig: 5.4 Interaction plot for Bearing Strength of S/N ratio

5.3.3 Optimal Design for Bearing Strength

The same level of all the significant factors provide a higher mean value and reduced variability so nothing has to be compromised. The level of factors which improves average and uniformity may conflict, so a compromise may have to be reached. Also compromise has to occur when multiple responses are considered and the same factor level may cause one response to improve and other to deteriorate.

In this experiment analysis, the main effect plot and interaction plot in Figure 5.1 and 5.2 used to estimate the mean bearing strength. From the Table 5.7 it is concluded that

highest bearing strength was observed at nanoclay content 2.0 wt% with twist drill geometry. Also, it was observed that there was no interaction between nanoclay and drill geometry. In S/N ratio highest bearing strength was found at nanoclay 2.0 wt% and at twist drill geometry.

Estimating the mean

Tensile strength is a "Higher the better" type response. In this experiment analysis, different experimental trials have been chosen to obtain satisfactory results. After conducting the experiments the optimum treatment condition within the experiments determined on the basis of prescribed combination of factor levels is determined to one of those in the experiment.

Mean value of bearing strength is given by:

$\mu_{C3D3} = C_3 + D_3 - T$ (Equation.... 5.2)

$= 84.13 + 78.19 - 87.13$

$= 75.19$ N/mm^2

Where T is given as mean bearing strength/no. of experiments.

Table 5.7: Significant factors and interactions

Factor	Affecting Mean		Affecting Variation	
	Contribution	Best Level	Contribution	Best Level
Feed (A)	Insignificant		Insignificant	
Speed (B)	Insignificant		Insignificant	
Nanoclay (C)	Significant	Level 2 (2.0 wt%)	Significant	Level 2 (2.0 wt%)
Drill Geometry (D)	Significant	Level 2 (Twist)	Significant	Level 2 (Twist)
C × D	Insignificant			Insignificant

Confidence Interval around the Estimated Mean

The confidence interval signifies the maximum and minimum value between which the true average should fall at some stated percentage of confidence. The estimate of the mean μ is only a point estimate based on the averages of results obtained from the

experiment. Statistically this provides a 50% chance of the true averages being greater than μ and a 50% chance of the true average being less than μ.

Confidence Interval around the estimated bearing strength mean

$$CI_1 = \sqrt{\left(F_{\propto,v_1,v_2} V_e\right)/\eta_{eff}}$$

Where $F_{\alpha}\, v_1 v_2$ = F ratio

α = risk (0.05)

confidence = 1- α

v_1 = dof for mean which is always = 1

v_2 = dof for error

$V_e = (SS_{total} - SS_{significant\ factors}) / (\text{total dof} - \text{dof of significant factors})$

η_{eff} = number of test under that condition using the participating factors

$\eta_{eff} = N/ (1+dof_{C,D)} = 18/(1+2+2) = 3.6$

$$CI_1 = \sqrt{\frac{4.67 \times 66.41}{3.6}} = 9.28$$

So the confidence interval level around the Bearing Strength is given by 75.19 ± 9.28 N/mm^2.

5.4 Results for Open-hole tensile test

The results for open hole tensile test for each of the 18 treatment conditions with repetition are given in Table 5.8. A confidence interval of 95% has been used for the analysis. The effects of parameters i.e. feed, speed, nanoclay, drill geometry were evaluated using ANOVA.

$$\text{Tensile Strength} = \frac{Peak\ Load}{(w-d)\times t} \qquad \text{(Equation...5.3)}$$

Where w = width of specimen (mm)

d = diameter of hole (mm)

t = thickness of specimen (mm)

Table 5.8: Results of specimens for Open hole Tensile test

Experiment No	Feed (mm/rev)	Speed (rpm)	Nanoclay (wt%)	Drill Geometry	Open hole test strength (N/mm^2)		Mean	S/N Ratio
					1	2		
1	Coarse	80	0.5	Step	405.6	348.0	376.8	51.52
2	Coarse	80	2.0	Twist	499	440.4	469.7	53.43
3	Coarse	80	3.0	Brad	431.4	400.0	415.7	52.37
4	Coarse	445	0.5	Step	340.0	383	361.5	51.16
5	Coarse	445	2.0	Twist	445.2	511.4	478.3	53.59
6	Coarse	445	3.0	Brad	459.1	399.5	429.3	52.65
7	Coarse	890	0.5	Twist	403.5	393.3	398.4	52.0
8	Coarse	890	2.0	Brad	416.5	482.9	449.7	53.05
9	Coarse	890	3.0	Step	417	420.8	418.9	52.44
10	Fine	80	0.5	Brad	400.3	354.9	377.6	51.54
11	Fine	80	2.0	Step	422.6	479.8	451.2	53.08
12	Fine	80	3.0	Twist	450.2	421.2	435.7	52.78
13	Fine	445	0.5	Twist	430.9	390.9	410.9	52.27
14	Fine	445	2.0	Brad	401.8	479.6	440.7	52.88
15	Fine	445	3.0	Step	449.2	366.8	408.0	52.21
16	Fine	890	0.5	Brad	387.6	393.8	390.7	51.83
17	Fine	890	2.0	Step	501.2	427.6	464.4	53.33
18	Fine	890	3.0	Twist	450.8	448.6	449.7	53.05

5.4.1 Analysis of Variance – Open hole tensile test

The results for tensile test were analyzed using ANOVA for identifying the significant factors affecting the performance measures. The Analysis of Variance (ANOVA) for the mean tensile test at 95% confidence interval is given in Table 5.9 The various data for each factor and their interaction was p value to find significant of each. The principal of the p value is that the value less than 0.05 that factors or interactions are significant if value is more than 0.05 then that factors or interactions are insignificant. From the ANOVA Table 5.9 it is seen nanoclay p value is 0.00, drill geometry p value

is 0.003 less than 0.05 so these factor are significant, other factors speed and feed has p value more than 0.05 so these factors are insignificant, same nanoclay and drill geometry (C×D) p value is 0.268 more than 0.05 so these factors are insignificant. In the table 5.8 shows the ranks of various factors in terms their relative significance. 1st rank is given to the nanoclay that mean nanoclay has the highest contribution to tensile strength. 2nd rank is given to the type of drill geometry, 3rd rank is given to the speed and the 4th rank is given to the feed that mean feed have the minimum contribution to the tensile strength.

Table 5.9: Analysis of Variance for means of Tensile test

Source	DOF	Seq SS	Adj MS	F	P	% Contribution	Status
Feed (A)	1	51.9	37.44	0.55	0.486	0.26	Insignificant
Speed (B)	2	216.8	139.31	2.05	0.210	1.09	Insignificant
Nanoclay (C)	2	16052.6	8026.31	118.04	0.000	81.28	Significant
Drill Geometry (D)	2	2558.2	1279.10	18.81	0.003	12.9	Significant
C × D	4	460.9	115.23	1.69	0.268	--	Insignificant
Residual Error	6	408.0	68.0	--	--	--	--
Total	17	19748.4	--	--	--	100	--

Table 5.10: Response Table for means of Tensile test

Level	Feed	Speed	Nanoclay	Drill Geometry
1	422.0	421.1	386.0	413.5
2	425.4	421.5	459.0	440.9
3	--	428.6	426.2	417.3
Delta	3.4	7.5	73.0	27.0
Rank	4	3	1	2

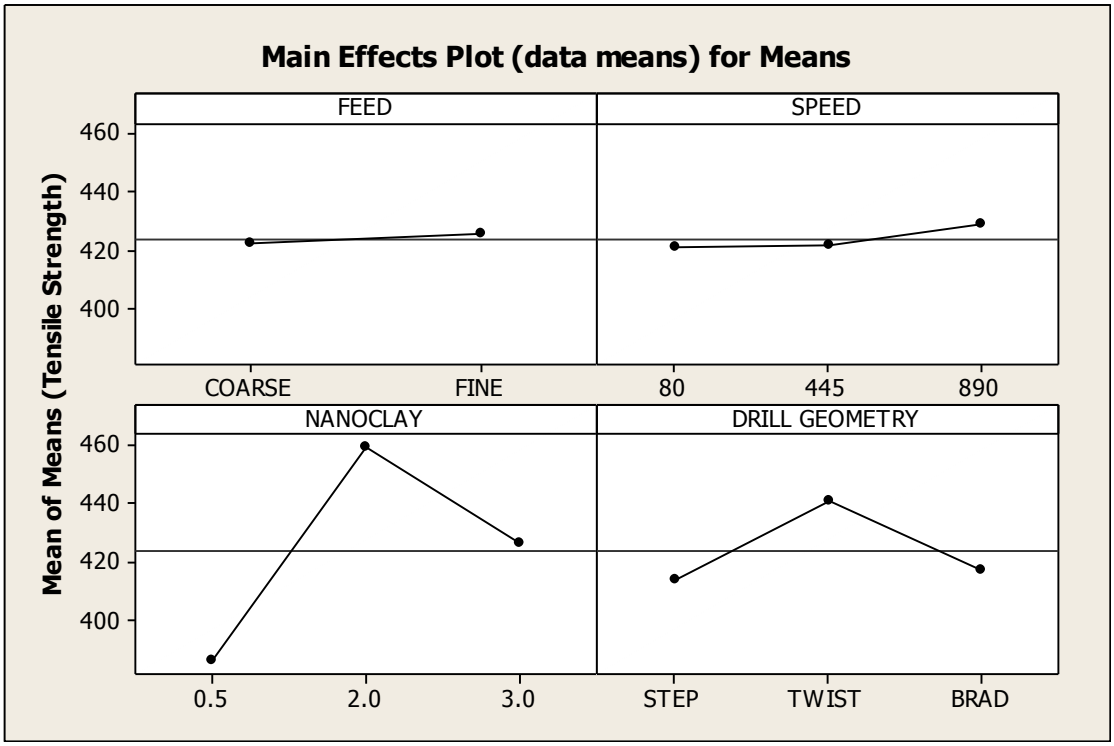

Fig: 5.5 Main effects plot of Tensile Strength for mean

In Figure 5.5 feed and speed have very small effect on tensile strength. There are two feed i.e. coarse and fine and three speed used 80, 445 and 890 rpm. Tensile strength increases with increase in nanoclay from 0.5 wt% to 2 wt%. Nanoclay having 0.5 wt% shows the minimum value of tensile strength, 2 wt% nanoclay give highest value of tensile strength and 3 wt% nanoclay give less tensile strength. Similarly twist drill give maximum tensile strength. Figure 5.6 shows the interaction between nanoclay and drill geometry for Mean.

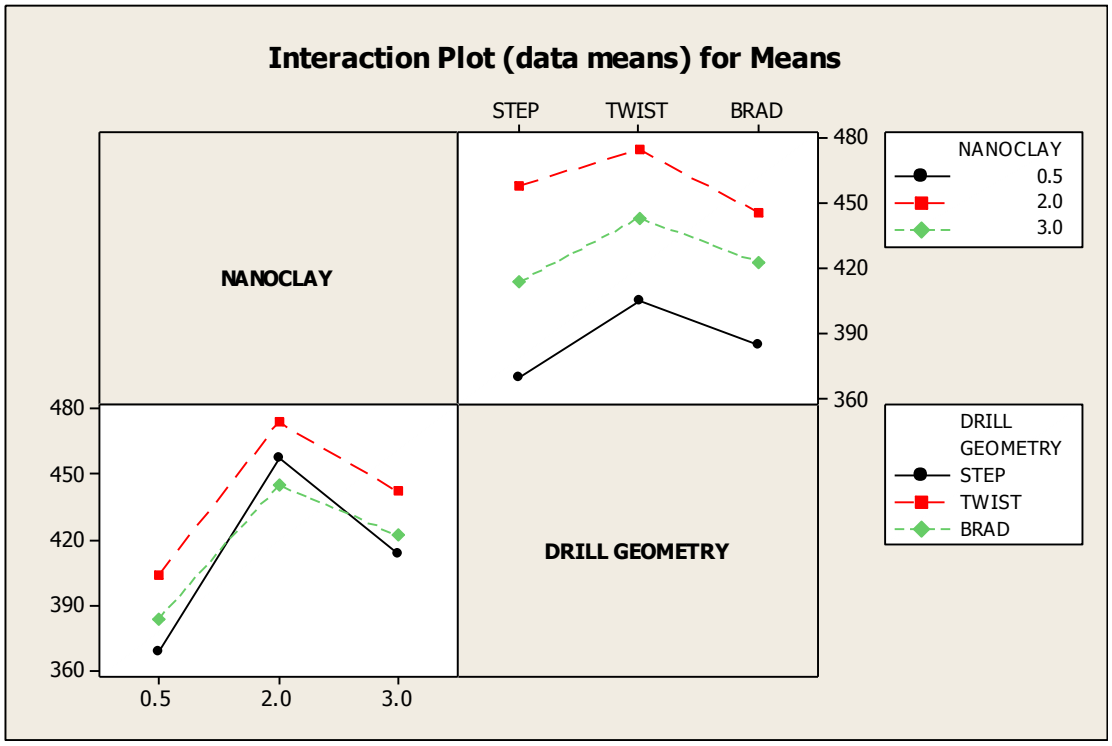

Fig: 5.6 Interaction plot of Tensile Strength for mean

5.4.2 Results for S/N ratio of tensile test

The S/N ratio consolidates several repetitions into one value and is an indication of the amount of variation present. The S/N ratios have been calculated to identify the major contributing factors and interactions that cause variation in the tensile test. Tensile test is "Higher is better" type response.

Table 5.11 shows the ANOVA results for S/N ratio of tensile test at 95% confidence interval. Nanoclay and drill geometry p values are less than 0.05 so these are significant factors. Feed and speed are insignificant factors having more p value. The interaction between nanoclay and drill geometry is insignificant. Table 5.12 show the ranks for different factors. Main effects plot and interaction plot of S/N ratio for tensile strength is shown in Figure 5.7 and 5.8.

Table 5.11: Analysis of Variance for S/N ratio of Tensile Strength

Source	DOF	Seq SS	Adj MS	F	P	% Contribution	Status
Feed (A)	1	0.03228	0.02048	0.65	0.453	0.38	Insignificant
Speed (B)	2	0.10615	0.05672	1.79	0.246	1.2	Insignificant
Nanoclay (C)	2	6.88047	3.44023	108.35	0.000	81.0	Significant

Drill Geometry (D)	2	1.09359	0.54680	17.22	0.003	12.8	Significant
C × D	4	0.19094	0.04774	1.50	0.312	--	Insignificant
Residual Error	6	0.19051	0.03175	--	--	--	--
Total	17	8.49394	--	--	--	100	--

Table 5.12: Response Table for S/N ratio of tensile strength

Level	**Feed**	**Speed**	**Nanoclay**	**Drill Geometry**
1	52.47	52.46	51.72	52.29
2	52.56	52.46	53.23	52.86
3	--	52.62	52.59	52.39
Delta	0.08	0.17	1.51	0.56
Rank	4	3	1	2

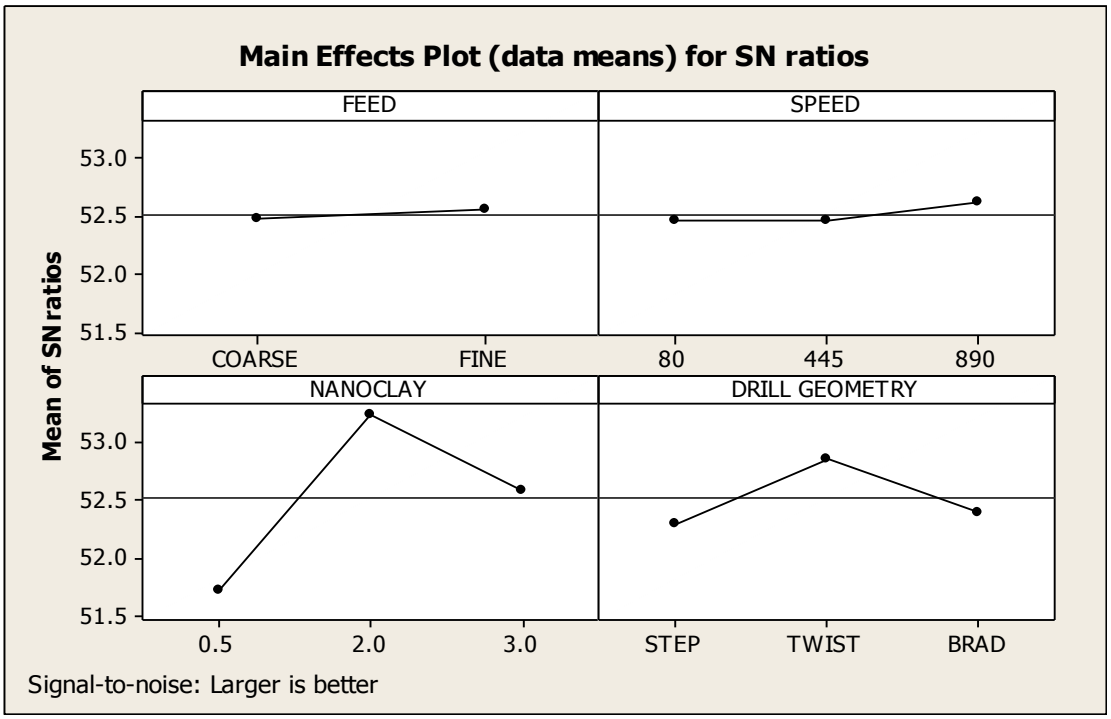

Fig: 5.7 Main effects plot of Tensile Strength for S/N ratio

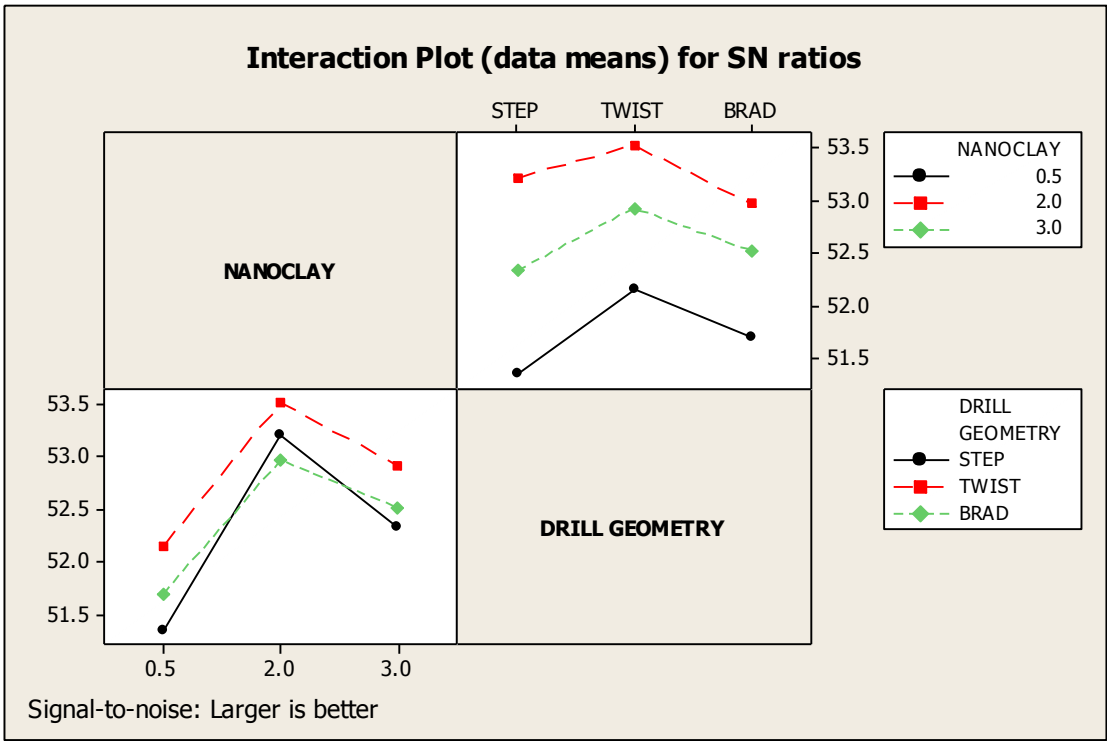

Fig: 5.8 Interaction plot of Tensile Strength for S/N ratio

5.4.3 Optimal Design for Tensile Strength

In this experiment analysis, the main effect plot and interaction plot in Figure 5.5 and 5.6 used to estimate the mean tensile strength. From the Table 5.13 it is concluded that highest tensile strength was achieved at nanoclay content of 2.0 wt%. and at twist drill geometry. Also, it was observed that there was no interaction between nanoclay and drill geometry. In S/N ratio highest tensile strength was found under same parameters.

Estimating the mean

Tensile Strength is a "Higher the better" type response. In this experiment analysis, different experimental trials have been chosen to obtain satisfactory results. After conducting the experiments the optimum treatment condition within the experiments determined on the basis of prescribed combination of factor levels is determined to one of those in the experiment.

Mean value of tensile strength is given by:

$\mu_{C3} = C_3 + D_3 - T$ (Equation....5.4)

$= 426.2 + 417.3 - 401.44$

$= 442.06\ N/mm^2$

Where T is given as mean tensile strength/no. of experiments.

Table 5.13 Significant factors and interactions

Factor	Affecting Mean		Affecting Variation	
	Contribution	Best Level	Contribution	Best Level
Feed (A)	Insignificant		Insignificant	
Speed (B)	Insignificant		Insignificant	
Nanoclay (C)	Significant	Level 2 (2.0 wt%)	Significant	Level 2 (2.0 wt%)
Drill Geometry (D)	Significant	Level 2 (twist)	Significant	Level 2 (twist)
C × D	InSignificant		InSignificant	

Confidence Interval around the Estimated Mean

The confidence interval signifies the maximum and minimum value between which the true average should fall at some stated percentage of confidence. The estimate of the mean μ is only a point estimate based on the averages of results obtained from the experiment.

Confidence Interval around the estimated tensile strength mean

$$CI_1 = \sqrt{\left(F_{\propto,V_1,V_2} V_e\right) / \eta_{eff}}$$

Where $F_{\alpha}\, v_1 v_2$ = F ratio

α = risk (0.05)

confidence = 1- α

v_1 = dof for mean which is always = 1

v_2 = dof for error

$V_e = (SS_{total} - SS_{significant\ factors}) / (\text{total dof} - \text{dof of significant factors})$

η_{eff} = number of test under that condition using the participating factors

$\eta_{eff} = N/ (1+dof_{C,D}) = 18/(1+2+2) = 3.6$

$$CI_1 = \sqrt{\frac{4.67 \times 89.07}{3.6}} = 10.74$$

So the confidence interval level around the Tensile Strength is given by 442.06 ± 10.74 N/mm^2.

5.5 Results for Delamination factor

The results for delamination of the 18 trials conducted in the experiment using L18 experimental design are given in Table 5.14. A confidence interval of 95% has been used for the analysis.

Delamination factor, $F_d = D_{max}/D$ (Equation..5.5)

Where D_{max} = maximum or damaged diameter of hole

D = nominal diameter of hole

Table 5.14: Results of specimens for Delamination factor

Experiment No	Feed (mm/rev)	Speed (rpm)	Nanoclay (wt%)	Drill Geometry	Delamination factor, Fd	Mean	S/N Ratio
1	Coarse	80	0.5	Step	1.10	1.10	-0.827
2	Coarse	80	2.0	Twist	1.05	1.05	-0.423
3	Coarse	80	3.0	Brad	1.20	1.20	-1.583
4	Coarse	445	0.5	Step	1.12	1.12	-0.984
5	Coarse	445	2.0	Twist	1.09	1.09	-0.748
6	Coarse	445	3.0	Brad	1.16	1.16	-1.289
7	Coarse	890	0.5	Twist	1.07	1.07	-0.587
8	Coarse	890	2.0	Brad	1.14	1.14	-1.138
9	Coarse	890	3.0	Step	1.08	1.08	-0.668
10	Fine	80	0.5	Brad	1.20	1.20	-1.583
11	Fine	80	2.0	Step	1.10	1.10	-0.827
12	Fine	80	3.0	Twist	1.06	1.06	-0.506
13	Fine	445	0.5	Twist	1.10	1.10	-0.827
14	Fine	445	2.0	Brad	1.09	1.09	-0.748
15	Fine	445	3.0	Step	1.07	1.07	-0.587
16	Fine	890	0.5	Brad	1.15	1.15	-1.213
17	Fine	890	2.0	Step	1.06	1.06	-0.506
18	Fine	890	3.0	Twist	1.09	1.09	-0.748

5.5.1 Analysis of variance – Delamination

The Analysis of Variance (ANOVA) for the mean delamination at 95% confidence interval is given in Table 5.15. The various data for each factor and their interaction was p value to find significance of each. The principal of the p value is that the value less than 0.05 that factors or interactions are significant if value is more than 0.05 then these are insignificant. From the ANOVA Table 5.15 it is seen drill geometry p value is 0.007 this factor is significant and other factors has p value more than 0.05 so these factors are insignificant, same nanoclay and drill geometry (C×D) p value is more than 0.05 so these factors are insignificant. In the Table 5.16 shows the ranks of various factors in terms their relative significance. 1st rank is given to the drill geometry that mean drill geometry has the highest effect on the delamination factor. 2nd rank is given to the type of nanoclay, 3rd rank is given to the speed and the 4th rank is given to the feed.

Table 5.15: Analysis of Variance for Means of Delamination

Cource	DOF	Seq SS	Adj MS	F	P	% Contribution	Status
Feed (A)	1	0.00045	0.000672	0.77	0.414	1.26	Insignificant
Speed (B)	2	0.00124	0.000333	0.38	0.698	3.48	Insignificant
Nanoclay (C)	2	0.00374	0.001872	2.15	0.198	10.50	Insignificant
Drill Geometry (D)	2	0.02441	0.011206	12.77	0.007	68.93	Significant
C × D	4	0.002278	0.000569	0.65	0.646	--	Insignificant
Residual Error	6	0.005233	0.000872		--	--	--
Total	17	0.035361	--	--	--	100	--

Table 5.16: Response Table for Means of Delamination

Level	Feed	Speed	Nanoclay	Drill Geometry
1	1.112	1.118	1.123	1.088
2	1.102	1.105	1.088	1.077
3	--	1.098	1.110	1.157
Delta	0.010	0.020	0.035	0.080
Rank	4	3	2	1

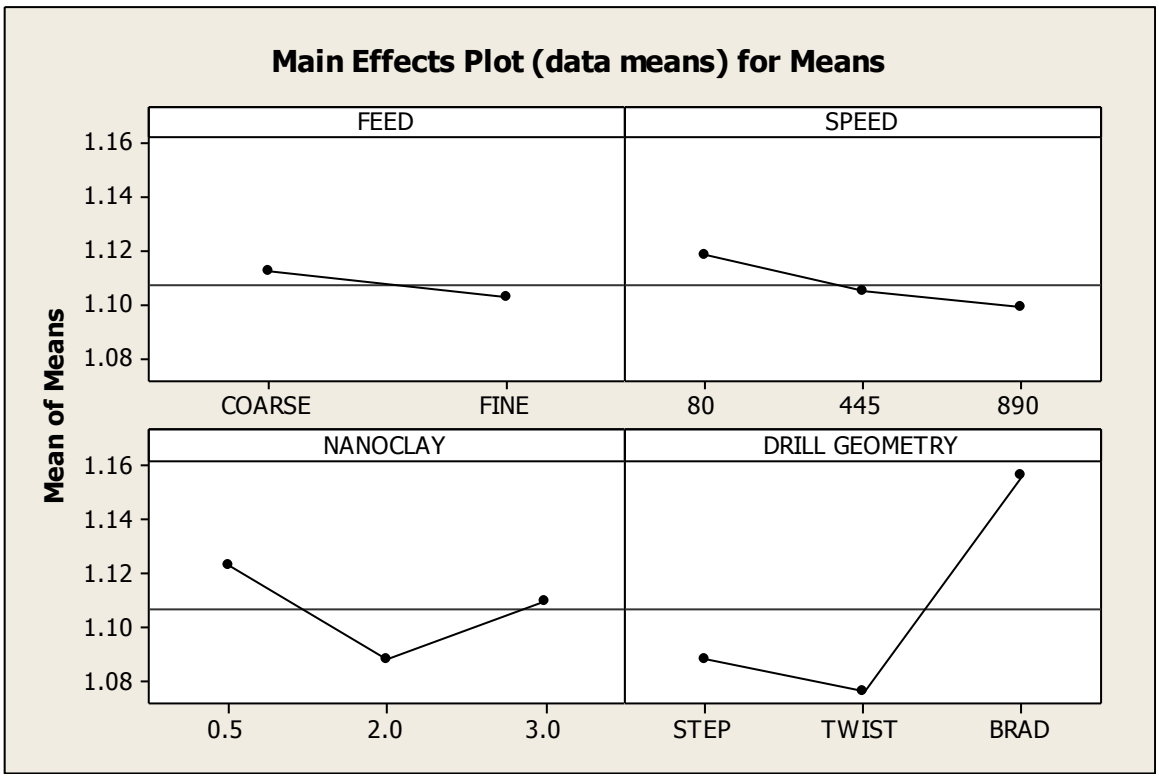

Fig: 5.9 Main effects plot of Delamination for means

In Figure 5.9 fine feed rate has small effect on delamination. With increase in speed from 80 to 890 rpm delamination decreases. Delamination also decreases with increase in nanoclay from 0.5 wt% to 2 wt%. Nanoclay having 0.5 wt% shows the more delamination, 2 wt% nanoclay give minimum value of delamination and 3 wt% nanoclay give less value. Similarly step drill give minimum delamination, twist drill

has least effect on delamination and the brad drill has maximum effect on delamination. Figure 5.10 shows the interaction plot of mean for delamination.

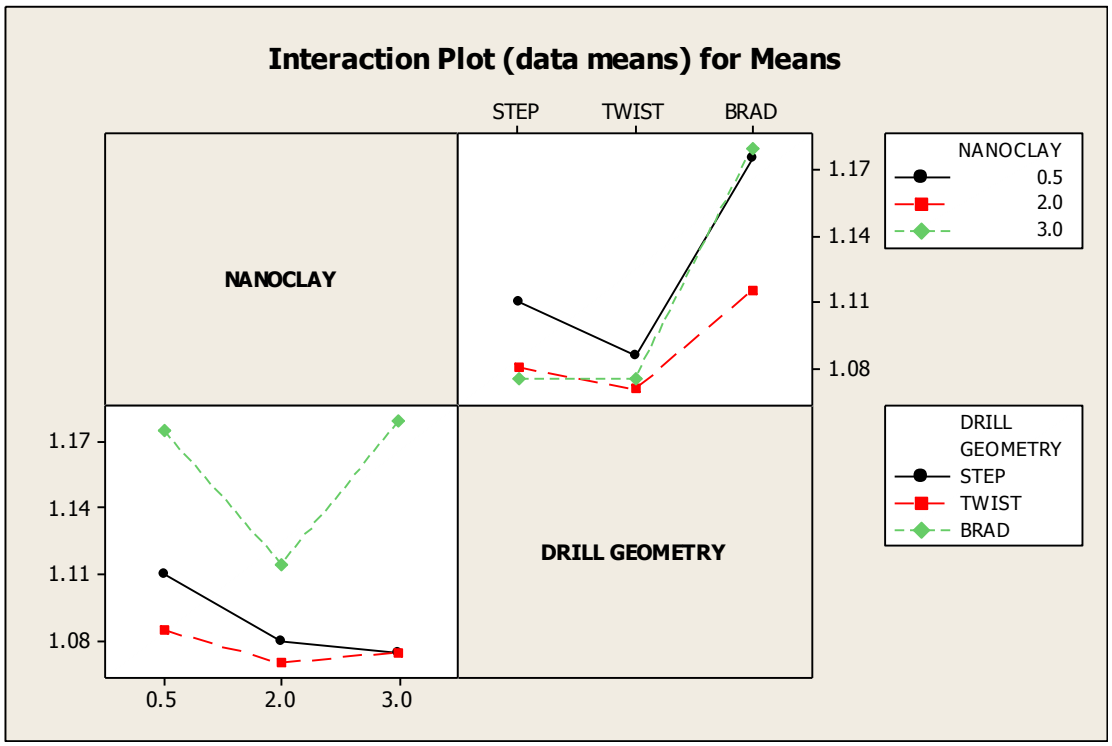

Fig: 5.10 Main effects plot of Delamination for interaction

5.5.2 Results for S/N ratio of Delamination

The S/N ratios have been calculated to identify the major contributing factors and interactions that cause variation in the delaminatione. Delamination factor is "Smaller is better" type response.

Table 5.17 shows the ANOVA results for S/N ratio of delamination factor at 95% confidence interval. Drill geometry is the factor which is found to be most significant affecting the delamination. Feed, speed and drill geometry are insignificant factors having more p value. The interaction between nanoclay and drill geometry is insignificant. Table 5.18 show the ranks for different factors. Main effects plot and interaction plot of S/N ratio for the delamination is shown in Figure 5.11 and 5.12.

Table 5.17 Analysis of Variance for S/N ratio of Delamination

Source	DOF	Seq SS	Adj MS	F	P	% Contribution	Status
Feed (A)	1	0.02732	0.04166	0.79	0.409	1.29	Insignificant
Speed (B)	2	0.06766	0.01971	0.37	0.704	3.30	Insignificant
Nanoclay (C)	2	0.22545	0.11272	2.13	0.200	10.68	Insignificant
Drill Geometry (D)	2	1.33682	0.66841	12.63	0.007	64.93	Significant
C × D	2	0.13512	0.03378	0.64	0.654	--	Insignificant
Residual Error	8	0.31754	0.05292		--	--	--
Total	17	2.10991	--	--	--	100	--

Table 5.18 Response Table for S/N ratio of Delamination

Level	Feed	Speed	Nanoclay	Drill Geometry
1	-0.9168	-0.9588	-1.0042	-0.7337
2	-0.8389	-0.8644	-0.7322	-0.6404
3	--	-0.8105	-0.8973	-1.2595
Delta	0.0779	0.1483	0.2721	0.6191
Rank	4	3	2	1

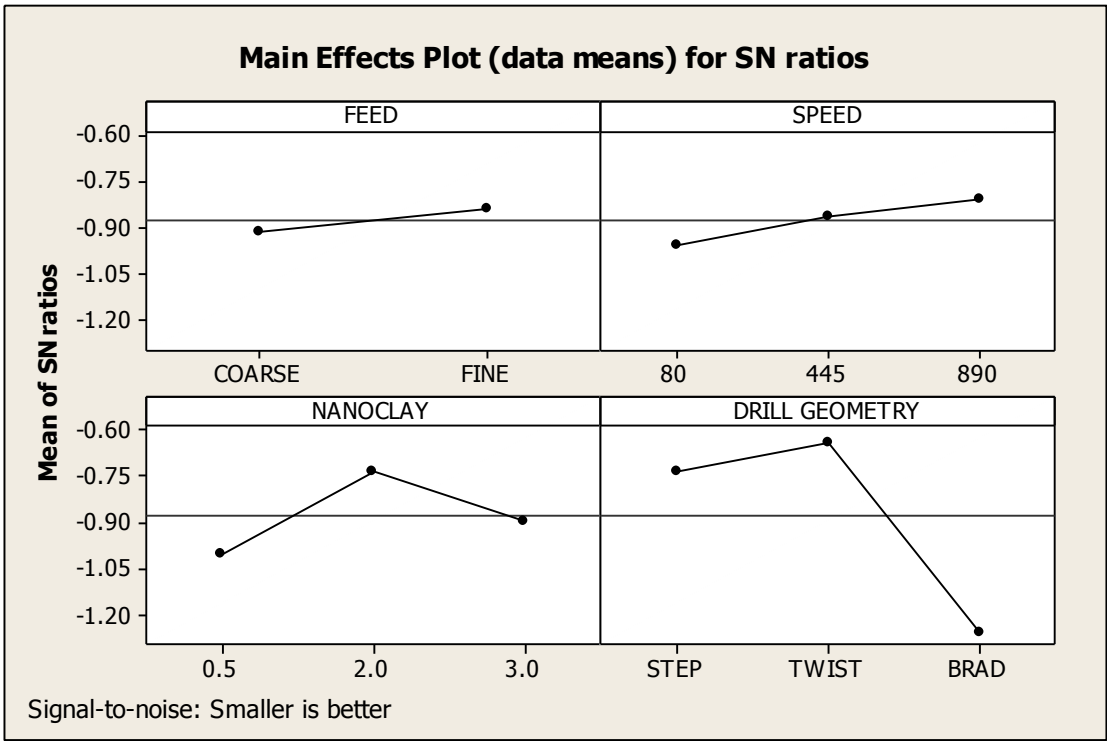

Fig: 5.11 Main effects plot of Delamination for S/N ratio

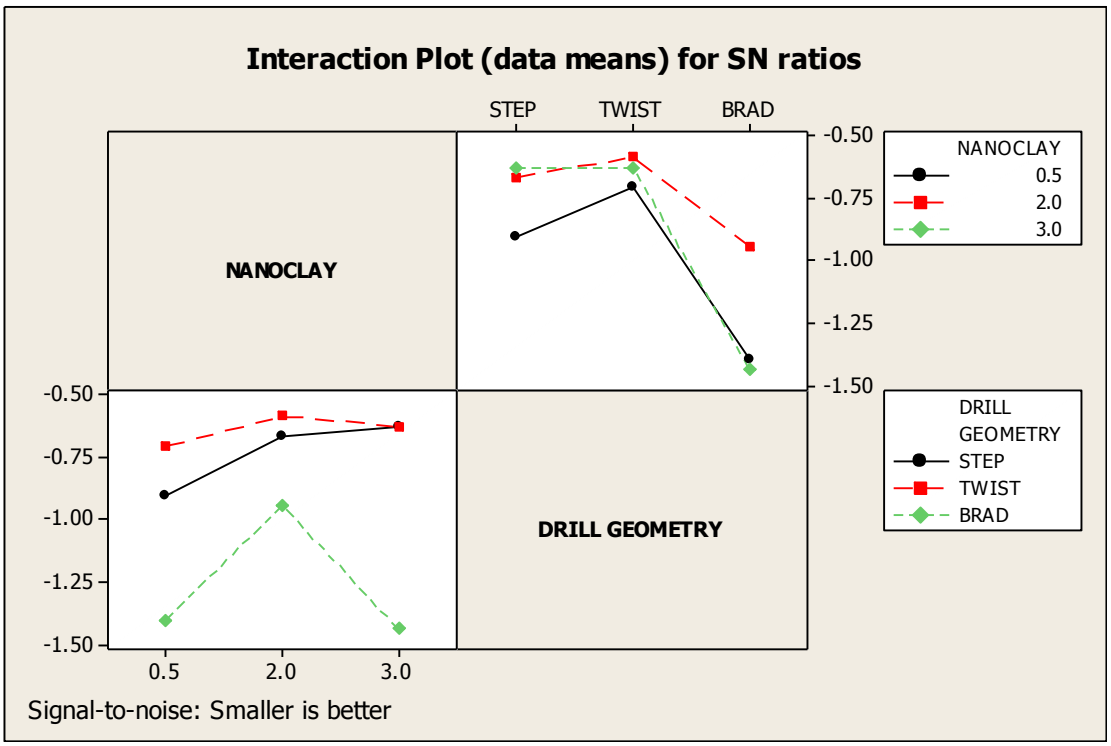

Fig: 5.12 Main effects plot of interaction for S/N ratio

5.4.3 Optimal Design for Delamination factor

In this experiment analysis, the main effect plot in Figure 5.9 used to estimate the mean Delamination factor. From the Table 5.19 it is concluded that minimum delamination was observed by using twist drill.

Estimating the mean

Delamination factor is a "Lower the better" type response. In this experiment analysis, different experimental trials have been chosen to obtain satisfactory results. After conducting the experiments the optimum treatment condition within the experiments determined on the basis of prescribed combination of factor levels is determined to one of those in the experiment.

Mean value of Delamination factor is given by:

$\mu_{D3} = D_3$ (Equation....5.5)

$= 1.157$

Table 5.19 Significant factors and interactions

Factor	Affecting Mean		Affecting Variation	
	Contribution	Best Level	Contribution	Best Level
Feed (A)	Insignificant		Insignificant	
Speed (B)	Insignificant		Insignificant	
Nanoclay (C)	InSignificant		InSignificant	
Drill Geometry (D)	Significant	Level 2 (twist)	Significant	Level 2 (twist)

Confidence Interval around the Estimated Mean

The confidence interval signifies the maximum and minimum value between which the true average should fall at some stated percentage of confidence. The estimate of the mean μ is only a point estimate based on the averages of results obtained from the experiment.

Confidence Interval around the estimated Delamination factor mean

$$CI_1 = \sqrt{\left(F_{\alpha,V_1,V_2} V_e\right) / \eta_{eff}}$$

Where $F_{\alpha} v_1 v_2$ = F ratio

α = risk (0.05)

confidence = 1- α

v_1 = dof for mean which is always = 1

v_2 = dof for error

$V_e = (SS_{total} - SS_{significant\ factors}) / (\text{total dof} - \text{dof of significant factors})$

η_{eff} = number of test under that condition using the participating factors

$\eta_{eff} = N/ (1+dof_{D)}) = 18/(1+2) = 6$

$$CI_1 = \sqrt{\frac{4.54 \times 0.0073}{6}} = 0.023$$

So the confidence interval level around the Delamination factor is given by 1.157 ± 0.023

6.1 Results

The effect of parameters i.e. feed, speed, nanoclay and drill geometry and interactions between nanoclay and drill geometry were evaluated using ANOVA design analysis. The purpose of the ANOVA was to identify the important parameters in prediction of bearing strength, residual tensile strength, delamination. Some results consolidated from ANOVA are given below:

6.1.1 Bearing Strength

A confidence interval of 95% has been used for the analysis. One repetition for each 18 trails was completed to measure the Signal to Noise ratio (S/N ratio).

From the ANOVA table for mean it is seen nanoclay p value is 0.00, drill geometry p value is 0.005 less than 0.05 which means these factors are significant. Speed and feed has p value more than 0.05 so these factors are insignificant, same nanoclay and drill geometry interaction p value is more than 0.05 so these factors are insignificant. The nanoclay was most significant factor and its contribution to bearing strength was 75.43% and the contribution of other significant factor i.e. drill geometry was 13.38%.

In the Table 5.4 show the rank of various factors in terms their relative significance. 1^{st} rank is given to the nanoclay that mean nanoclay has the highest contribution to bearing strength. 2^{nd} rank is given to the type of drill geometry, 3^{rd} rank is given to the feed and the 4^{th} rank is given to the speed that mean speed have the minimum contribution to the bearing strength.

The highest bearing strength was observed at nanoclay content 2.0 wt% with twist drill geometry. Also, it was observed that there was no interaction between nanoclay and drill geometry. In S/N ratio highest bearing strength was found at nanoclay 2.0 wt% and at twist drill geometry.

With 95% confidence interval mean value of bearing strength was found to be 75.19 ± 9.28 N/mm^2.

6.1.2 Tensile Strength

A confidence interval of 95% has been used for the analysis. One repetition for each 18 trails was completed to measure the Signal to Noise ratio (S/N ratio).

From the ANOVA table it is seen nanoclay p value is 0.00 less than 0.05 so this factor is significant and their contribution to tensile strength was 81.28%, so 1st rank is given to the nanoclay, drill geometry p value is 0.02 less than 0.05 so this factor is also significant and their contribution to tensile strength was 12.9% so 2nd rank is given to the type of drill geometry. Speed and feed has p value more than 0.05 these factors are insignificant, same nanoclay and drill geometry (C×D) interaction p value is more than 0.05 so these factors are insignificant. Nanoclay has the highest contribution to tensile strength. The highest tensile strength was observed at nanoclay content 2.0 wt%. In S/N ratio highest tensile strength was found at nanoclay 2.0 wt%.

With 95% confidence interval mean value of tensile strength was found to be 447.6 ± 10.74 N/mm^2.

6.1.3 Delamination factor

A confidence interval of 95% has been used for the analysis. From the ANOVA table 5.15 it is seen drill geometry p value is 0.007 this factor is significant and other factors has p value more than 0.05 so these factors are insignificant, same nanoclay and drill geometry (C×D) interaction p value is more than 0.05 so these factors are insignificant. In the table 5.16 shows the ranks of various factors in terms their relative significance. 1st rank is given to the drill geometry which signifies that it provides the highest contributionon to the delamination factor. 2nd rank is given to the type of nanoclay, 3rd rank is given to the speed and the 4th rank is given to the feed. Drill geometry has more contribution for delamination i.e. 63.93%. In S/N ratio, lowest delamination was observed at drill geometry. Twist drill was found to be most affective drill having lowest delamination factor.

With 95% confidence interval mean value of tensile strength was found to be 1.157 ± 0.023.

6.2 Conclusions

By adding the nanoclay from 0.5 wt% to 2 wt % the hardness of the specimen increased. At 2 wt% nanoclay the sample was the hardest among all the compositions and on further increasing the nanoclay content i.e. at 3 wt% hardness starts decreasing. Residual bearing strength and tensile strength is mainly affected by nanoclay and drill geometry. The maximum bearing and tensile strength is obtained at nanoclay content of 2 wt%. When nanoclay content increased to 3 wt% the strength of specimens decreased. The use of twist drill geometry increases the tensile and bearing strength. Delamination factor has affected mostly by drill geometry. With the use of twist drill minimum delamination was observed.

Also with increasing speed from 80 to 890 rpm and at low feed rate of fine delamination factor decreases.

6.3 Future Scope

1. To see the effect of nanofillers on FRP`s, experiments can be repeated by changing the type of nanofillers.
2. The experiment can be done by using different composition of the nano filler.
3. The present work can be extended with different diameter of drill bit, different types of drill geometry with more number of drills, process parameters, material thickness.

REFERENCES

1. **H. Hocheng and C.C. Tsao. "**Comprehensive analysis of delamination in drilling of composite materials with various drill bits", *Journal of Materials Processing Technology* , vol. 140 , pp. 335-339, March 2003.
2. **U.A. Khashaba, I. El-Sonbaty and T. Machaly. "**Factors affecting the machinability of GFR/epoxy composites", *Composite structures*, vol. 63, pp. 329-338, 2004.
3. **H. Hocheng and C.C. Tsao. "**The path towards delamination-free drilling of composite materials", *Journal of Materials Processing Technology*, vol. 167, pp. 251-264, 2005.
4. **Antonio T. Marques, Luis M. Durao, Antonio G. Magalhaes, Joao Francisco Silva, Joao, Manuel R. S. Tavares.** "Delamination Analysis of Carbon fiber Reinforced Laminates: Evaluation of a special Step drill", reference PTDC/EME-TME/66207, 2006.
5. **Luis Miguel P. Durao, Daniel J. S. Gonçalves, Joao Manuel R. S. Tavares, Victor Hugo C. de Albuquerque, A. Torres Marques.** "Comparative Analysis of drills for composite Laminates", reference PTDC/EME-TME/66207, 2006.
6. **Antonio T. Marques, Luis M. Durao and Antonio G. Magalhae. "**Delamination analysis of carbon fiber reinforced laminates", *Composite materials,* 2007.
7. **A.M. Abrao, P.E. Faria, J.C. Campos Rubio and P. Reis.** "Drilling of fiber reinforced plastics: A review", *Journal of Materials Processing Technology*, vol.186, pp. 1-7, November 2007.
8. **C.C. Tsao. "**Taguchi analysis of drilling quality associated with core drill in drilling of composite material", *International Advanced manufacturing techonology*, vol. 877-884, pp. 877-884, March 2007.
9. **C.C. Tsao. "**Thrust force and delamination of core-saw drill during drilling of carbon fiber reinforced plastic (CFRP)', *International Advanced manufacturing techonology*, vol. 23-28, pp. 23-28, February 2007.
10. **V.N. Gaitonde, S.R. Karnik, J. Campos Rubio, A. Esteves Correia, A.M. Abra O, J. Paulo Davim.** "Analysis of parametric influence on delamination in

high-speed drilling of carbon fiber reinforced plastic composites", *Journal of materials processing technology*, vol. 203, pp.431-438, 2008.

11. **Luis M. Durao, Antonio T. Marques, Antonio G. Magalhaes b, Joao Francisco Silva and Joao Manuel R.S. Tavares.** "Delamination analysis of carbon fiber reinforced laminates:Evaluation of a special step drill", *Composites Science and Technology*, vol. 69, pp. 2376-2382, 2009.
12. **David Aspinwall, Islam Shyha, Sein Leung Soo and Sam Bradley.** "Effect of laminate configuration and feed rate on cutting performance when drilling holes in carbon fibre reinforced plastic composites", *Journal of Materials Processing Technology*, vol. 210, pp.1023-1034, 2009.
13. **I. Singh, R.A. Kishore, R. Tiwari and A. Dvivedi.** "Taguchi analysis of the residual tensile strength after drilling in glass fiber reinforced epoxy composites", *Materials and Design*, vol.30, pp. 2186–2190, 2009.
14. **P.K. Rakesh, I. Singh, D. Kumar.** "Failure prediction in glass fiber reinforced plastics laminates with drilled hole under uni-axial loading", *Materials and Design*, vol.31, pp. 3002–3007, 2010.
15. **L.M.P. Durao, D.J.S Goncalves, J.M.R.S. Tavares, V.H.C. de Albuquerque and A. Torres Marques.** "Drilling process of composite Laminates – A tool based Analysis", *European conference on composite materials*, paper ID: 184-ECCM 14, 2010.
16. **Luis Miguel P. Durao, Joao Manuel R.S. Tavares, Victor Hugo C. de Albuquerque and Daniel J.S. Gonçalves.** "Damage evaluation of drilled carbon/epoxy laminates based on area assessment methods", *Composite Structure*, 2012.
17. **Vaibhav A. Phadnis, Farrukh Makhdum, Anish Roy and Vadim V. Silberschmidt.** 'Experimental and numerical investigations in conventional and ultrasonically assisted drilling of CFRP laminate', Procedia CIRP, vol.1 , pp.455-459, 2012.
18. **T.V. Rajamurugan, K. Shanmugham, K. Palanikumar.** "Analysis Of Delamination In Drilling Glass Fiber Reinforced Polyester Composites", *Materials and Design*, vol.12, pp.0261-3069, 2012.
19. **Luis Miguel P. Durao, Joao Manuel R.S. Tavares, Victor Hugo C. de Albuquerque, Daniel J.S. Gonçalves.** "Damage evaluation of drilled

carbon/epoxy laminates based on area assessment methods", *Composites Structures*, 2012.

20. **Vijayan Krishnaraj, A. Prabukarthi, Arun Ramanathan, N. Elanghovan, M. Senthil Kumar, Redouane Zitoune, J.P. Davim.** "Optimization of machining parameters at high speed drilling of carbon fiber reinforced plastic (CFRP) laminates", *Composites*, vol. 43, pp.1791-1799, January 2012.
21. **DeFu Liu, YongJun Tang, W.L. Cong,** "A review of mechanical drilling for composite laminates", *Composite structures*, vol-94, pp.1265-1279, November 2012.
22. **T.J. Grilo, R.M.F. Paulo, C.R.M. Silva, J.P. Davim.** "Experimental delamination analyses of CFRPs using different drill geometries", *Composites*, vol. 45, pp.1344-1350, August 2013.
23. **Metin Krabult.** A Thesis report on "Production and characterization of nano composites material from recycled thermoplastics", thesis submitted by Metin Krabult.
24. **Gurdyal Singh.** A Thesis report on "Damage detection and evaluation in glass fibre reinforced polymer laminated composites",
25. **Vistasp M Karbhari.** A Thesis report on "Methods of detecting defects in composites rehabilitated concrete structures", Department of Structural Engineering, University of California, San Diego, 2005.
26. http://en.wikipedia.org/wiki/File:Schema_MEB.
27. **Luis Miguel P. Durao, Joao Manuel R.S. Tavares, Victor Hugo C. de Albuquerque, Daniel J.S. Gonçalves.** 'Damage evaluation of drilled carbon/epoxy laminates based on area assessment methods', *Composites Structures*, 2012.
28. Delamination in drilling GFR-thermoset composites, composite structure, vol 63 (2004).